Advances in Nano Research, *Vol. 10, No. 3 (2021) 295-312*
DOI: https://doi.org/10.12989/anr.2021.10.3.295

Ionic liquid coated magnetic core/shell $CoFe_2O_4@SiO_2$ nanoparticles for the separation/analysis of trace gold in water sample

Yanxia Zeng*[1,2], Xiashi Zhu[1], Jiliang Xie[2] and Li Chen[2]

[1]*Department of Chemical Engineering, Yangzhou University, Yangzhou City, Jiangsu Province, 225009, China*
[2]*Institute of Marine Resource Development, Jiangsu Ocean University, Lianyungang, Jiangsu Province, 222005, China*

(*Received December 8, 2020, Revised January 25, 2021, Accepted February 3, 2021*)

Abstract. A new ionic liquid functionalized magnetic silica nanoparticle was synthesized and characterized and tested as an adsorbent. The adsorbent was used for magnetic solid phase extraction on ICP-MS method. Simultaneous determination of precious metal Au has been addressed. The method is simple and fast and has been applied to standard water and surface water analysis. A new method for separation/analysis of trace precious metal Au by Magnetron Solid Phase Extraction (MSPE) combined with ICP-MS. The element to be tested is rapidly adsorbed on $CoFe_2O_4@SiO_2$@[BMIM]PF6 composite nano-adsorbent and eluted with thiourea. The method has a preconcentration factor of 9.5-fold. This method has been successfully applied to the determination of gold in actual water samples. Hydrophobic Ionic Liquids (ILs) 1-butyl-3-methylimidazole hexafluorophosphate ([BMIM]PF6) coated $CoFe_2O_4@SiO_2$ nanoparticles with core-shell structure to prepare magnetic solid phase extraction agent ($CoFe_2O_4@SiO_2$@ILs) and establish a new method of MSPE coupled with inductively coupled plasma mass spectrometry for separation/analysis of trace gold. The results showed that trace gold was adsorbed rapidly by $CoFe_2O_4@SiO_2$@[BMIM]PF_6 and eluanted by thiourea. Under the optimal conditions, preconcentration factor of the proposed method was 9.5-fold. The linear range, detection limit, correlation coefficient (R) and relative standard deviation (RSD) were found to be 0.01~1000.00 ng·mL^{-1}, 0.001 ng·mL^{-1}, 0.9990 and 3.4% (n = 11, c = 4.5 ng·mL^{-1}). The $CoFe_2O_4@SiO_2$ nanoparticles could be used repeatedly for 8 times. This proposed method has been successfully applied to the determination of trace gold in water samples.

Keywords: gold; magnetic silica nanoparticles; magnetic solid phase extraction; [BMIM] PF_6; loaded

1. Introduction

Precious metals gold (Au) is widely applied in many industry fields due to the high catalytic activity, excellent corrosion resistance, and good electrical conductivity (Reuter *et al*. 2016, Vojoudi *et al*. 2017, Chen *et al*. 2018a, Deng *et al*. 2020, Xu *et al*. 2020b). Although precious metals have many applications and advantages in biological systems, their high levels in human cells are toxic (Inoue *et al.* 2015, He *et al.* 2017, Chang 2020, Jiao *et al.* 2020, Jiao *et al.* 2020, Roy *et al.* 2020, Wang *et al.* 2020). Therefore, removal of precious metals gold (Au) from water resources at trace level is of the paramount importance (Cheng *et al*. 2016, He *et al*. 2018a, b, Shen *et al*. 2020). A variety of techniques have been used for pre-concentration and separation of metal ions including liquid-liquid extraction, ion exchange, co-precipitation, solid-phase extraction (Aziz-Zanjani *et al*. 2014, Radi *et al*. 2014, Amiri *et al*. 2017a, b, Liu *et al*. 2020b, Qi and Fourie 2019, Qi *et al.* 2019, Qi *et al*. 2020, Qi *et al.* 2020, Qi *et al*. 2020). For example, in order to eliminate the time-consuming and costly process of experimental investigations, different optimization approaches have been suggested (Moghaddam *et al*. 2009, Fanaie *et al*. 2012, 2015a, b, 2016a, b, Fanei and Dizaj 2014). In recent decades, researchers have focused on novel methods for data prediction and estimation. In this regard, soft computing and computational techniques have been proposed which have many applications in different fields including education, medical diagnosis, engineering, transportation and so on (Mohammadhassani *et al*. 2013, 2014, Safa *et al*. 2016, 2020, Sadeghipour Chahnasir *et al*. 2018, Sedghi *et al*. 2018, Katebi *et al*. 2019, Mansouri *et al*. 2019, Milovancevic *et al*. 2019, Shariati *et al*. 2020, Toghroli *et al*. 2014, Toghroli *et al*. 2016, Shariati *et al*. 2019, Shariati *et al*. 2019, Trung *et al*. 2019). Soft computing approaches are based on techniques such as fuzzy logic, artificial neural network, genetic algorithm and machine learning (Ha *et al.* 2018, Ganesan *et al*. 2020, Shariati *et al*. 2019, Shariati *et al*. 2019, Safa *et al*. 2020, Shariati *et al*. 2020, Shariati *et al*. 2020, Yazdani *et al*. 2020). It should be mentioned that the accuracy of these methods have been proved in numerous studies (Ha *et al*. 2018, Tran *et al*. 2018a, b, Takizawa *et al*. 2019, Ahamed *et al*. 2020, Arif *et al*. 2020, Bazilevs *et al*. 2020, Nguyen-Thi *et al*. 2020, Pho and Truong 2020, Takizawa *et al*. 2020, Pham *et al*. 2021, Dinh-Cong *et al*. 2019, Alaskar *et al*. 2020, Alaskar *et al*. 2020, Alyousef *et al*. 2020, Cao *et al*. 2020, Cao *et al*. 2020, Cao *et al*. 2020, Cao *et al*. 2020, Huang *et al*. 2020, Liu *et al*. 2020). Among these technologies, magnetic micro-spheres and

*Corresponding author, Ph.D.,
E-mail: yojohhit@126.com

ISSN: 2287-237X (Print), 2287-2388 (Online)

nanoparticles have been attracting more and more attention for enrichment and separation in trace elements (Awual 2016, Amiri *et al*. 2017a, Gao and Lu 2020). MFe_2O_4 (M stands for metal element) is a magnetic material having a cubic spinel structure and is widely used and widely used in many fields (Chen *et al*. 2017, 2018b, Mehdinia *et al*. 2017, Gao *et al*. 2021). Among them, $CoFe_2O_4$ has a high saturation magnetization, good adsorption capacity, magnetic recovery ability and heat stability higher than room temperature, and has become a hot magnetic core material in magnetic solid phase extraction in recent years (Chen *et al*. 2010, Zhu *et al*. 2017, Afrazi 2018, Wang *et al*. 2018a, Mou *et al*. 2019, Shi *et al*. 2020). In the past few years, various magnetic solid phase extraction techniques using $CoFe_2O_4$ as a magnetic core have been reported for the study of the removal of metal ions from aqueous solutions (He *et al*. 2018c, Liu *et al*. 2018, Lu *et al*. 2019, Yang *et al*. 2020b, Zhang *et al*. 2020k, Qi *et al*. 2020, 2021). The accurate, sensitive and quick detection of the trace gold in waste water is very significant (Li *et al*. 2020b, Liu *et al*. 2020c, Zhang *et al*. 2020h, j). Therefore, a new method of Magnetic Solid Phase Extraction (MSPE) coupled with ICP-MS for separation/ analysis of trace precious metal Au adsorbed rapidly on $CoFe_2O_4$@SiO_2@[BMIM]PF_6 and eluted with thiourea was established (Long *et al*. 2015, Zhu *et al*. 2018a, Deng *et al*. 2019, Zhang *et al*. 2019c). This method has been successfully applied to the determination of Au in real water samples (Hu *et al*. 2019, Wu *et al*. 2019, Zhu *et al*. 2019b, 2020a).

2. Experimental

2.1 Reagents

All reagents were of analytical grade or higher in purity and purchased from Sinopharm Chemical Reagent Co., Ltd. (Shanghai, China), unless otherwise specified. Milli-Q water (Millipore, Bedford, MA, USA) was used throughout the study. Britton-Robinson (B-R) buffer solutions were prepared by blending the mixed acid (0.04 mol/LH_3PO_4, HAc and H_3BO_3) with 0.2 mol/L NaOH in proportion. PQ was obtained from the Chinese National Institute for the Control of Pharmaceutical and Biological Products (Beijing, China) without further treatment (Tsai *et al*. 2019, Zhu *et al*. 2019a, Jia *et al*. 2021). N-methylimidazole (Darui Fine Chemicals, Shanghai, China), N-butyl bromide, 1-Bromohexane, 1-Bromooctane, tetraethyl orthosilicate (TEOS), KPF_6, $FeCl_3$, $(NH_4)_2Fe(SO_4)_2$, ethanol, acetone, methylene chloride (Sinopharm Chemical Reagent Co., Ltd., Shanghai, China) (Zuo *et al*. 2015, Zhong *et al*. 2020).

2.2 Apparatus

All pH values were measured by a PHS-25B pH meter (Shanghai Precision & Scientific Instrument Co., Ltd., Shanghai, China) (Zuo *et al*. 2017, Feng *et al*. 2020b, Yu *et al*. 2020b). FT-IR spectra were measured with a Bruker Tensor 27 spectrometer (Bruker company, Germany). Samples were pressed into KBr pellets and recorded at the frequencies from 4000 to 400 cm^{-1} with resolution of 4 cm^{-1} (Afrazi and Dehghani 2014, Afrazi and Rouhanifar 2019, Afrazi *et al*. 2017, 2018a, b, Afrazi *et al*. 2019, Majedi *et al*. 2020a, b, Rouhanifar *et al*. 2020). The trace elements analysis was performed by Inductively coupled plasma mass spectrometer ICP-MS M90 (Bruker Company, Germany). The pH value was adjusted by a PHS-25B pH meter (Shanghai Precision & Scientific Instrument Co., Ltd., Shanghai, China). X-ray direction (XRD) pattern was collected by a X'Pert Pro diractometer (PANalytical, Netherlands) (Feng *et al*. 2020a, Tian *et al*. 2020). Magnetization measurement was studied by an MPMS-7 vibrating sample magnetometer (VSM) (Quantum Design, USA) (Liu *et al*. 2015, Lu *et al*. 2020).

2.3 Preparation of $CoFe_2O_4$@SiO_2@[BMIM]PF_6 MNPs

Cobalt Ferrite Nanoparticles ($CoFe_2O_4$ NPs) were prepared by the conventional hydrothermal method (Rahimi *et al*. 2018). First, $Co(NO_3)_2{\cdot}6H_2O$ (2.27 g) was dissolved in ethylene glycol (250 mL) followed by addition of $Fe(NO_3)_3{\cdot}9H_2O$ (6.30 g) and of anhydrous sodium acetate (11.25 g) under stirring (Liu *et al*. 2017, Huang *et al*. 2020). Then polyethylene glycol (6.250 g) was added rapidly under vigorous stirring (Wu *et al*. 2020). The resultant solution was stirred (1000 $r{\cdot}min^{-1}$ 1) at 50°C for 30 min, and then the suspension was transferred to a reaction kettle, and reacted at 200°C for more than 16 h. After cooling to room temperature, the obtained $CoFe_2O_4$ precipitate was centrifuged for 10 min at 10000 $r{\cdot}min^{-1}$ and then the precipitate was collected and washed with deionized water and ethanol for more than 3 times, and subsequently the $CoFe_2O_4$ NPs was dried at 60°C for 6 h in vacuum, and then transferred to a muffle (Xu *et al*. 2020c). The black precipitate was calcined at 500°C for 10 min and then ground stored (Singh *et al*. 2011, Han *et al*. 2020, Yang *et al*. 2020c). $CoFe_2O_4$@SiO_2 core-shell particles was prepared according to a modified Stober method (Stöber *et al*. 1968, Lu *et al*. 2008). $CoFe_2O_4$ NPs (0.100 g) were dissolved in 120 mL ethanol and 30 mL deionized water by sonication for 30 min, and then 10 mL ammonium hydroxide, 1 g CTAB dispersant and 1.00 mL TEOS were added sequentially (Qian *et al*. 2020b). The mixture was reacted for 12 h at 40°C under a continuous stirring (Qian *et al*. 2020a). The resultant product was collected by an external magnetic field, and rinsed with deionized water and ethanol for six times thoroughly, and dried in vacuum to obtain $CoFe_2O_4$@SiO_2 NPs. The preparation of hydrophobic ionic liquid (ILs) 1-butyl-3-methylimidazole hexafluorophosphate ([BMIM]PF_6) was prepared using the following methods (Fang *et al*. 2008, Chen *et al*. 2015). A 250 mL three-necked flask containing an equimolar amount (0.05 mol) of 1-bromobutane (or 1-bromo-n-hexane), N-methylimidazole and KPF_6 was stirred and refluxed in a water bath at 80°C. Condensation for 3.5 h. After cooling to room temperature, 10 mL of deionized water was added and the mixture was separated into an upper aqueous phase and a lower [C_4MIM][PF_6] ionic liquid phase (Zhang *et al*.

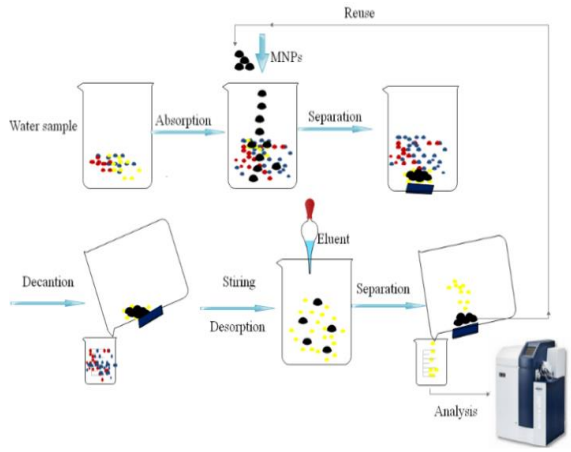

Fig. 1 Schematic of MSPE procedure for detecting gold (III) content using $CoFe_2O_4$@SiO_2@[BMIM]PF_6

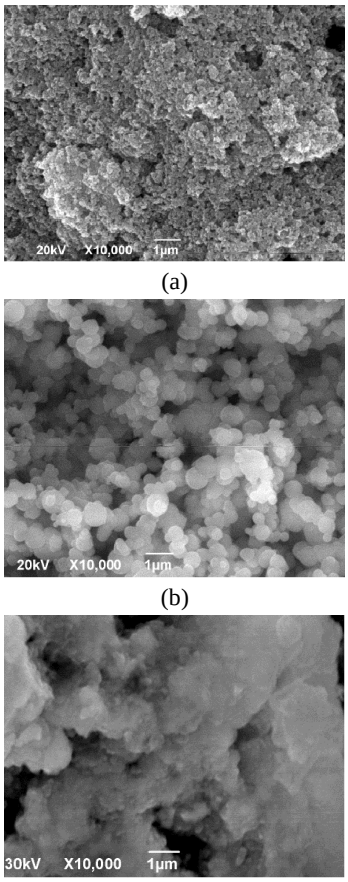

Fig. 2 SEM micrographs of (a) $CoFe_2O_4$, (b) $CoFe_2O_4$ @SiO_2 and (c) $CoFe_2O_4$ @SiO_2@[BMIM]PF_6 (Wang *et al*. 2019)

2020e, f). The ionic liquid phase was washed with a certain amount of deionized water until Br-complete removal (checking whether Br- remained with $AgNO_3$ solution) and washing with diethyl ether (15 mL×3). Finally, it was vacuum dried at 120°C for 2 h to obtain a pale yellow oily room temperature ionic liquid [C_4MIM][PF_6] (Hu *et al*. 2020). ILs functionalized $CoFe_2O_4$@SiO_2@[BMIM]PF_6 (CSIL MNPs) were synthesized following a procedure described the literature (Dang *et al*. 2012). 0.400 g [BMIM] PF_6 was dissolved in 60.0 mL acetonitrile, and then 0.300 g $CoFe_2O_4$@SiO_2 nanoparticles were added. Stir the mixture in the fume hood until the acetonitrile completely evaporated (Zuo *et al*. 2013, Li *et al*. 2020c). The obtained CSIL MNPs functionalized material was washed with methylene chloride, and dried at 60°C under vacuum for 12 h. The solid was carefully grinded into powders, which were CSIL MNPs.

2.4 MSPE procedure

The general extraction procedure is illustrated in Fig. 1. A 2.00 ml of 10 ug·g^{-1} gold (III) standard solution or aqueous sample solution, 0.50 ml 0.2 mol·L^{-1} potassium iodide solution, 2.0 ml of BR buffer (pH=4.00) solution and 0.01 g of CSIL MNPs were sequentially added to a centrifuge tube, and the solution in the tube was subsequently shaken in the constant temperature shaking table for 3 min at room temperature. Then the CSIL MNPs with adsorbed target gold (III) was gathered and kept static for 0.5 min with an externally applied Nd-Fe-B permanent magnet. Once the suspension became limpid, the supernatant was pipetted out. The isolated CSIL MNPs were eluted with 3.0 mL 1.5% thiourea+1 M hydrochloric acid to elute the preconcentrated target analytes for 20 min. The eluted solution was collected and made up to volume, and the target analyte was detected by ICP-MS. The whole time of the process was about 30 min. The general extraction procedure is illustrated in Fig. 1.

2.5 Sample preparation

Water sample was collected from several reservoirs and springs in Lianyungang city, China. A 50.0 mL of lake water sample was filtered through 0.45 um membrane to remove suspended particles before analysis. The samples were stored at −4°C in a refrigerator. The residual gold (III) content in the supernatants was determined by measuring signal value of ^{195}Au by ICP-MS.

2.6 Characterization of the MNPs

The crystal structure of the MNPs sample was carried out on a Rigaku X-ray diffractometer (XRD) with Cu K radiation in the range of 20 to 80° and a scanning speed of 10°/min. The TEM image was obtained from HITACHI 7000FA with an accelerating voltage of 100 kV. The surface morphology of CSIL MNPs was examined by SEM (JEOL, 6300 LA). The composition was examined by energy dispersive spectroscopy (EDS) in FE-SEM. UV-visible absorption (UV-2450, SHIMADZU) was recorded using a spectrophotometer. The magnetic properties of the nanoparticles were determined using a 4HF vibrating sample magnetometer (VSM). The surface properties and composition of the particles were investigated by Fourier transform infrared (FTIR) spectroscopy (Thermo Nicolet, Nexus FTIR spectrometer, KBr pellets, in the range of 400-4000 cm^{-1}). Samples were evaluated by Raman spectroscopy in the range of 200-3500 cm^{-1} using a 514.5

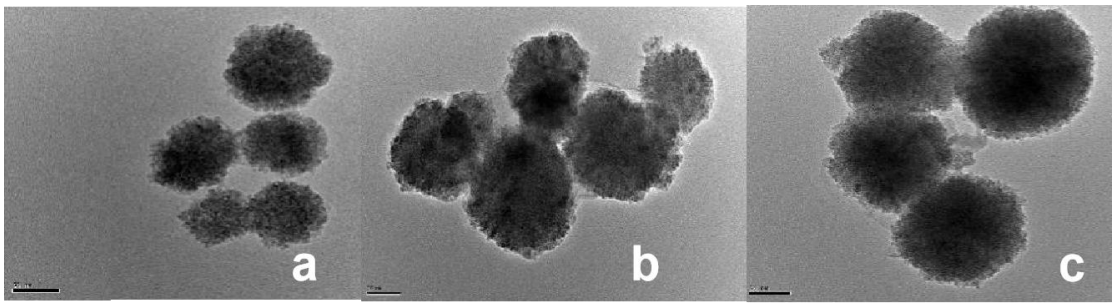

Fig. 3 TEM micrographs of (a) $CoFe_2O_4$, (b) $CoFe_2O_4$ @SiO_2 and (c) $CoFe_2O_4$@SiO_2@[BMIM]PF_6 (Wang *et al*. 2018b).

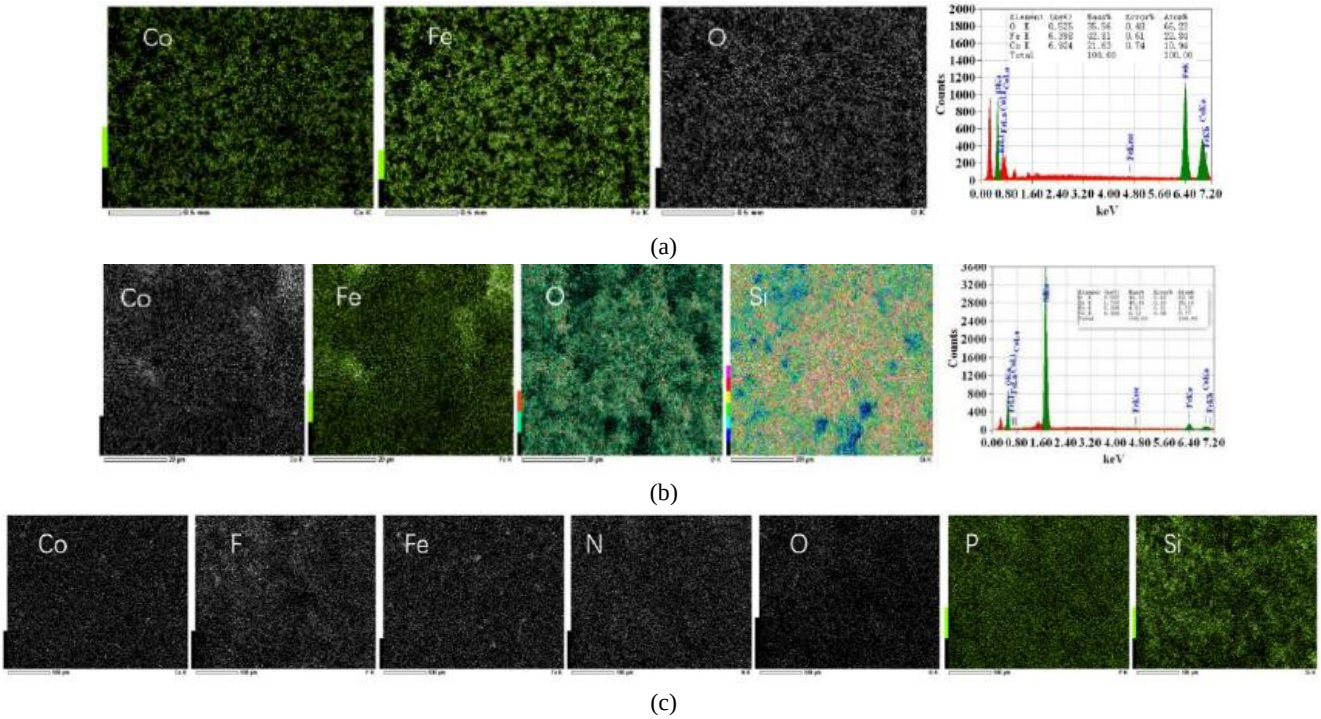

Fig. 4 Elemental analysis of NPs by energy dispersive X-ray (EDX) analysis. (a) $CoFe_2O_4$, (b) $CoFe_2O_4$@SiO_2, (c) $CoFe_2O_4$ @SiO_2@[BMIM]PF_6 nanoparticles (Zhang *et al*. 2020d)

nm line from a hydrogen ion laser. The hydrodynamic diameter and zeta potential were measured by a Zetasizer (Malvern 3000 HSA). The TG-DTA measurement was carried out on a Netzsch heat balance STA 409 PC / PG type, heated to 900°C at room temperature, and raised at a rate of 10°C/min in an air atmosphere. Specific surface area measurement using N_2 adsorption using an analyzer, X-ray photoelectron spectroscopy (XPS), nuclear magnetic resonance (NMR).

3. Results and discussion

3.1 Preparation and characterization of the MNPs

Preparing of $CoFe_2O_4$ nanoparticles was carried out by the one-step hydrothermal method in an aqueous medium.So the reaction was carried out as in the equations below (Sun *et al*. 2020b)

$$2Fe^{3+} + Co^{2+} \rightarrow Fe_2Co\,(OH)_8 \quad (1)$$

$$Fe_2Co(OH)_8 \rightarrow CoFe_2O_4 + 4H_2O \quad (2)$$

Cobalt iron oxide nanoparticles surface modified by the process Silanization. This reaction involves the covering of a surface cobalt iron oxide nanoparticles through self-assembly with (3-aminopropyl)- triethoxy silane molecules (Liu *et al*. 2019, Wu *et al*. 2020). During this reaction, hydroxyl groups on the surface of iron oxide nanoparticles attack and replace ethoxy groups of APTES, thus is formed a covalent -Si-O-Si- bond and amino propyl-terminated surface. The surface coating of nanoparticles by APTES depends on experimental parameters like silane concentration, temperature and reaction time (Ju *et al*. 2020, Liu *et al*. 2020a, Wei *et al*. 2020).

3.1.1 SEM and TEM analysis

The SEM and TEM images of $CoFe_2O_4$, $CoFe_2O_4$@SiO_2 and $CoFe_2O_4$@SiO_2@[BMIM]PF_6 are shown in Figs. 2 and 3, separately (Jia *et al*. 2020b).

As shown in Fig. 2, the improved hydrothermal synthesis of $CoFe_2O_4$ NPS particles has a typical spherical

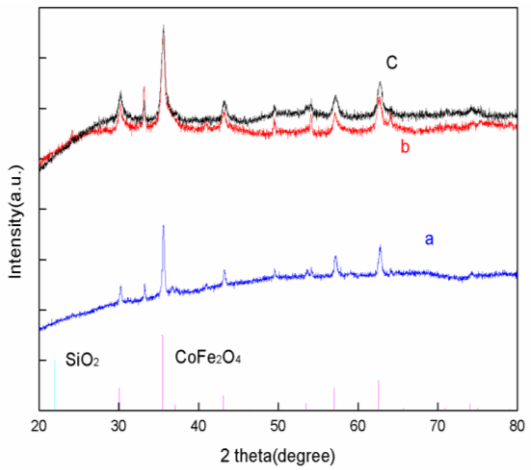

Fig. 5 XRD spectra of (a) $CoFe_2O_4$, (b) $CoFe_2O_4@SiO_2$, (c) $CoFe_2O_4@SiO_2@[BMIM]PF_6$ (Zhang *et al*. 2020a)

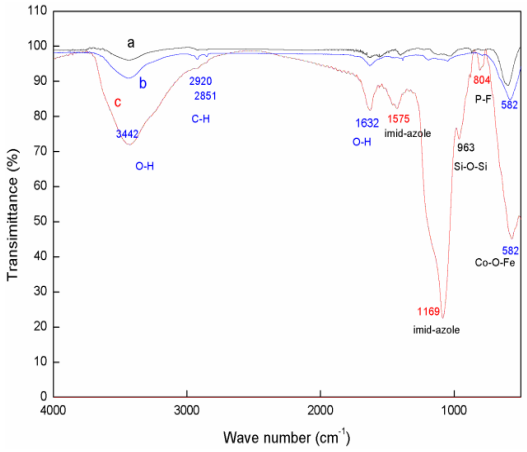

Fig. 6 FTIR spectra of (a) $CoFe_2O_4$, (b) $CoFe_2O_4@SiO_2$, (c) $CoFe_2O_4@SiO_2@[BMIM]PF_6$ (Zhang *et al*. 2020a)

structure with a nano-scale material size between 50 and 60 nm, while $CoFe_2O_4@SiO_2$ displays a relatively compact structure with a bigger nano-scale size between 100 and 200 nm. Moreover, $CoFe_2O_4@SiO_2@[BMIM]PF_6$ MNPs shows dense and homogeneous morphology and no obvious interface is observed, revealing the good compatibility between $CoFe_2O_4@SiO_2$ and $[BMIM]PF_6$ ionic liquid, which is beneficial for improving the adsorption performance of CSIL composites (Chen *et al*. 2010, Wang *et al*. 2020f). The typical core-shell structure of the silica gel nanoparticles can be seen by transmission electron microscopy and the boundary between the particles becomes unclear after the ionic liquid is loaded (Abedini *et al*. 2020b, Zhang *et al*. 2020b).

3.1.2 EDX analysis

The elemental composition of the $CoFe_2O_4$, $CoFe_2O_4@SiO_2$ and $CoFe_2O_4@SiO_2@[BMIM]PF_6$ nanoparticles were estimated by using an EDX detector and the results were shown in Figs. 4(a)-(c). The energy spectrum results show that Fig. 4(a) contains three elements Co, Fe, O with a Co/Fe ratio of 1:2, Fig. 4(b) contains Co, Fe, O, Si and the Si content reaches 20%, and Fig. 4(c) contains two other elements N, F, indicating that $[BMIM]PF_6$ is successfully loaded on the $CoFe_2O_4@SiO_2$ nanoparticles (Alam *et al*. 2020a, Zhu *et al*. 2020b).

3.1.3 XRD analysis

Phase investigation of the crystallized product was performed by XRD analysis for the $CoFe_2O_4$ NPs and APTES coated nanoparticles as presented in Figs. 5(a)-(c).

XRD results show that a typical $CoFe_2O_4$ crystal phase magnetic core (a) is prepared and the $CoFe_2O_4$ crystal phase is a cubic spinel structure (JCPDS card: 22-1086). The intensity of the crystallization peak of this sample is relatively weak and wide, indicating crystallinity. Low and particle size, which may result in low stability of the resulting material. Panel (b) and (c) shows no significant SiO_2 peak in the XRD pattern, indicating that the SiO_2 coated on the $CoFe_2O_4$ NPs is amorphous (Alam *et al*. 2020b, Zhang and Mousavi 2020).

3.1.4 Characterization by FTIR

The surface nature of samples was qualitatively assessed before and after salinization and Ionic liquid functionalization step by using FTIR spectroscopy and the results were shown in Fig. 6(a)-(c). Fig. 6 was shown the FTIR spectra of $CoFe_2O_4$ (curve a), $CoFe_2O_4@SiO_2$ (curve b), $CoFe_2O_4@SiO_2@$ [BMIM] PF_6 (curve c). Compared the curves of a and b, a peak of 582 cm^{-1} was assigned to Co–O–Fe stretching vibration; the strong peaks of 963 $cm^{-1}$and 1084 cm^{-1} correspond to the Si–O–H and Si–O–Si stretching vibration; which indicated that SiO_2 had been successfully loaded on the surface of $CoFe_2O_4$. In the curve c, the peaks at 2920 cm^{-1} and 2851 cm^{-1} corresponded to the C–H stretching vibration, the peaks at 3442 cm^{-1} and 1632 cm^{-1} corresponded to the O–H stretching vibration and the bending vibration of water molecules, the peaks at 1575 cm^{-1} corresponded to the characteristic absorption of imid-azole groups in the $CoFe_2O_4@SiO_2@BMIM]PF_6$; in addition, the peak of 804 cm^{-1} was attributed to the P–F stretching vibration in the $CoFe_2O_4@SiO_2@[BMIM]PF_6$, which indicated that the $[BMIM]PF_6$ ion liquids had been successfully immobilized on the surface of $CoFe_2O_4@SiO_2$.

3.1.5 Thermogravimetric analysis

Thermogravimetric analysis (TGA) revealed the weight loss process of the materials, which indicated the difference between the $CoFe_2O_4@SiO_2$ and $CoFe_2O_4@SiO_2@$ $[BMIM]PF_6$. In this paper, TGA was conducted in a nitrogen atmosphere, and the heating rate employed was 10°C ·min^{-1}, all cases from 35 to 880°C (Fig. 7). The experimental results could be concluded that (1) After heating from 120°C to 260°C, the mass loss of $CoFe_2O_4$, $CoFe_2O_4@-SiO_2$ and $CoFe_2O_4@SiO_2@[BMIM]PF_6$ was about 0.64%, 10.84%, 8.21%, respectively, corresponding to the water content; (2) For the $CoFe_2O_4@SiO_2$ $@[BMIM]PF_6$, an additional weight loss of 23.28% was observed with respect to the mass loss of $CoFe_2O_4@SiO_2$ of 9.91% after heating from 260°C to 350°C due to decomposition of $[BMIM]PF_6$. This observation suggested

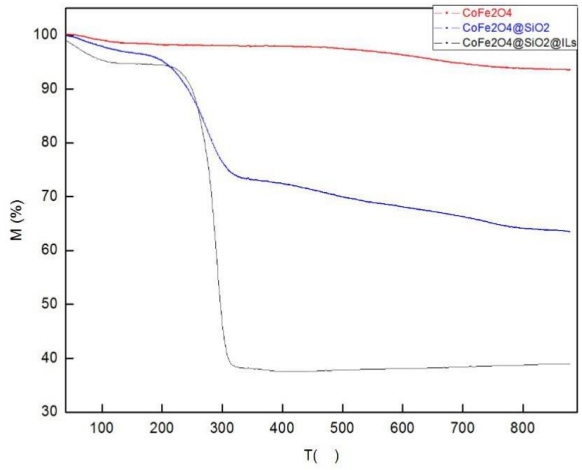

Fig. 7 TGA spectra of (a) $CoFe_2O_4$, (b) $CoFe_2O_4$@SiO_2, (c) $CoFe_2O_4$@SiO_2@[BMIM]PF_6

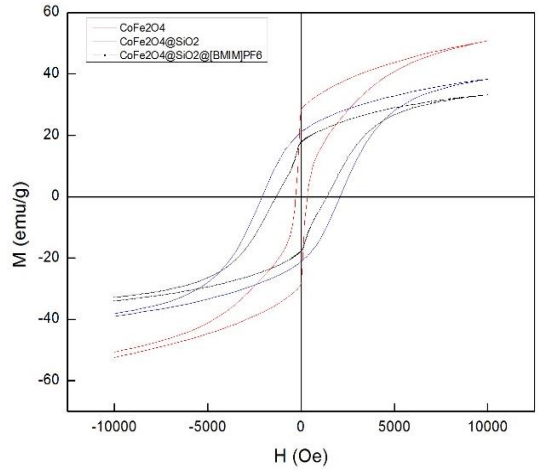

Fig. 8 Magnetization at 10 K as a function of magnetic field for (a) $CoFe_2O_4$(a), (b) $CoFe_2O_4$@SiO_2, (c) $CoFe_2O_4$@SiO_2@[BMIM]PF_6, respectively (Zhang *et al*. 2019b)

Table 1 Magnetic property analysis of the MNPs and the high-magnetic field part of the M(H) curves obtained by VSM measurements

MNPs	Ms (emug)	Mr (emu/g)	H/Oe
$CoFe_2O_4$	28.68	28.24	780
$CoFe_2O_4$@SiO_2	21.12	21.10	4000
$CoFe_2O_4$@SiO_2@[BMIM]PF_6	17.90	17.7	1200

Fig. 9 Attracting magnetite nanoparticles of (a) $CoFe_2O_4$, (b) $CoFe_2O_4$ @SiO_2 and (c) $CoFe_2O_4$ @SiO_2@[BMIM]PF_6 by a magnet (Zhang *et al*. 2019c)

that the ion liquids [BMIM] PF_6 had been located on the surface of $CoFe_2O_4$@SiO_2.

3.1.6 Magnetic characterization

Using a magnetometer at 27°C indicated that the maximal saturation magnetizations of $CoFe_2O_4$, $CoFe_2O_4$ @SiO_2 and $CoFe_2O_4$@SiO_2@[BMIM]PF_6 MNPs were 28.68, 21.12 and 17.90 emu·g^{-1} shown in Table 1, respectively. The decrease of maximal saturation magnetizations of $CoFe_2O_4$@SiO_2@[BMIM]PF_6 MNPs resulted from the nonmagnetic SiO_2 and ion liquids shell (Alam *et al*. 2020c, Li *et al*. 2020a). Fig. 8 described the magnetic hysteresis loops of the three MNPs, and it was apparent that all of the NPs show superparamagnetic properties in the presence of magnetite particles in the core (Sun *et al*. 2019a, Zhang and Wang 2019b).

The saturation magnetization of 16.3 $emug^{-1}$ was sufficient for magnetic separation with a magnet, though the saturation magnetization of $CoFe_2O_4$ decreased after coating SiO_2 and [BMIM]PF_6 (Wang *et al*. 2011, Zhang *et al*. 2019a). Therefore, the $CoFe_2O_4$@SiO_2@[BMIM]PF_6 MNPs prepared here could be rapidly separated from solution with a magnet on account of their superparamagnetic and large saturation magnetization, as it is shown in Fig. 9.

3.2 Optimizations of gold (III) extraction

To optimize the extraction procedure of gold (III), we focused on the following factors: pH, the ionic strength, oscillation time, adsorption temperature, the extraction time, the amount of $CoFe_2O_4$@SiO_2@[BMIM]PF_6 and the sample volume (Sun *et al*. 2018, Gholipour *et al*. 2020a).

3.2.1 Effect of pH

PH is a crucial factor affecting the extraction efficiency of gold (III). In this work, the effect of pH was investigated over the range of 4.0 to 9.0. The effect of pH was investigated by varying the pH values between 1.0 and 9.0 (Fig. 10(a)). The experimental results showed that pH had significant impact on the adsorption efficiency of Au (III), and the optimum value is 4.0. The extraction rate of gold (III) % increased with the pH and reached plateau between the pH ranges of 1.0-4.0 while increased with the pH between the ranges of 4.0-9.0. Therefore, pH 4.0 was selected for the subsequent assays (Zhu *et al*. 2018b, Sun *et al*. 2019b). The extraction rate of the system decreases sharply with the increase of pH when the pH of the solution is greater than 4.0, which is mainly due to the hydrolysis of $[AuCl_4]^-$ as the pH of the system increases. In addition, removal of $[AuCl_4]^-$ from aqueous solutions is effective due to the effects of ion-ion interactions ($[BMIM]^+$ and $[AuCl_4]^-$ interactions) and the hydrogen bonding interactions (hydrogen bonding between anion and the imidazole ring C_2-H) (Kordestani *et al*. 2020a, b).

3.2.2 Effect of ionic strength

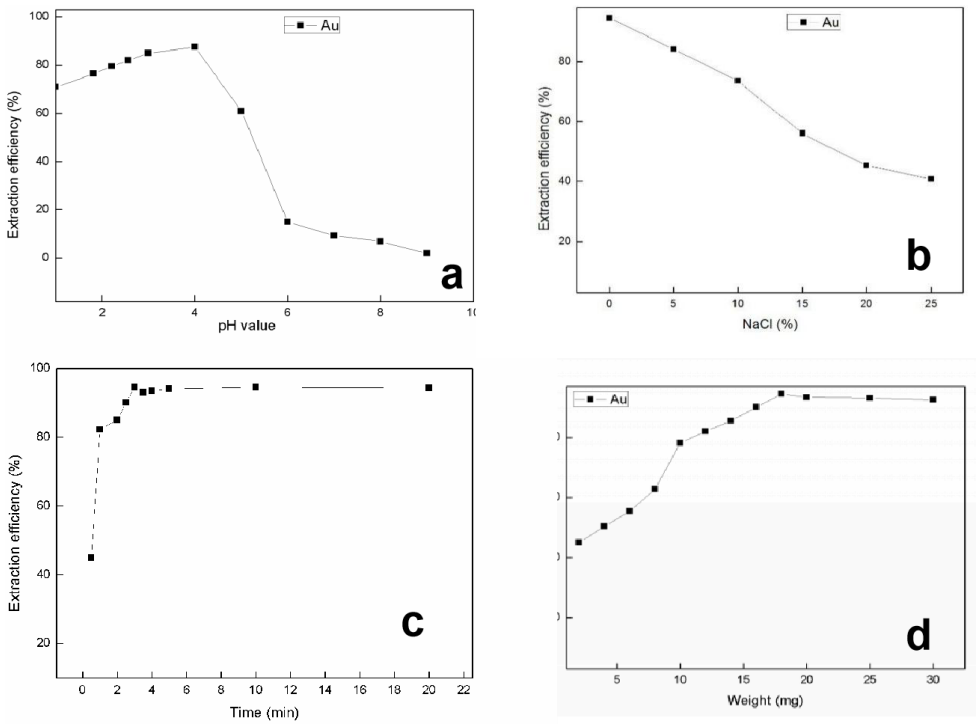

Fig. 10 Effect of (a) pH, (b) ionic strength, (c) adsorption temperature and (d) sample volume on extraction rate of trace gold (III) by $CoFe_2O_4$@SiO_2@[BMIM]PF_6($Conc_{Au(III)}$=25.0 μg/mL)

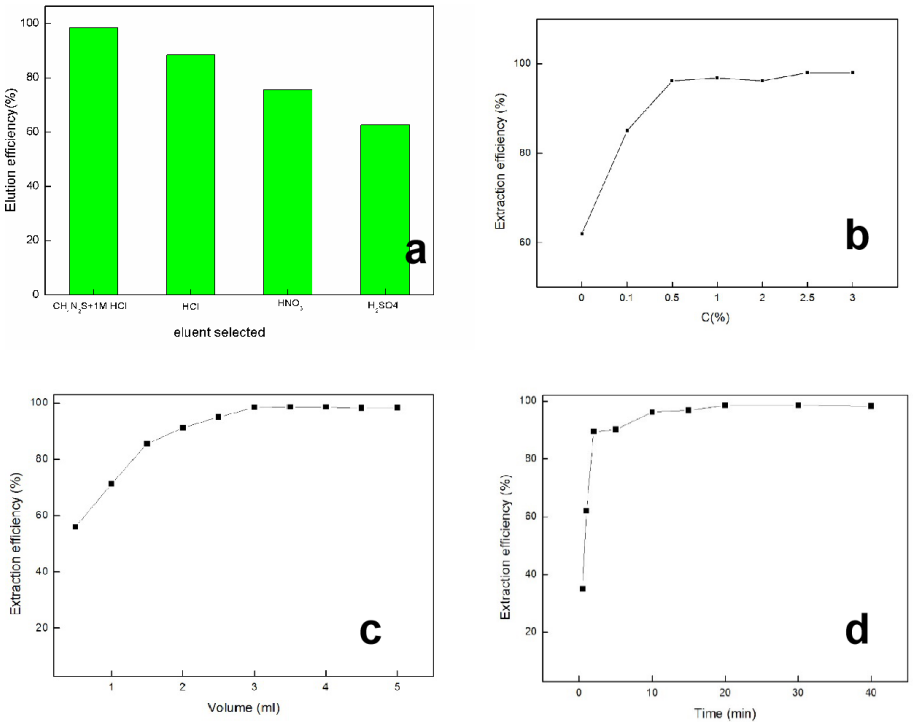

Fig. 11 Effect of (a) eluent selected, (b) eluent concentration, (c) eluent volume and (d) elution time on elution efficiency of gold (III) absorbed by $CoFe_2O_4$@SiO_2@[BMIM]PF_6 ($Conc_{Au(III)}$ = 25.0μg·mL^{-1})

The effect of ionic strength was evaluated in the concentration range of 0-25% (w/v) using sodium chloride as the model electrolyte (Fig. 10(b)). With the increase of NaCl concentration, the adsorption efficiency of gold (III) gradually decreases, which is mainly due to the competitive adsorption of chloride ions because of increase of NaCl concentration, which leads to the decrease of adsorption efficiency. In addition, when the NaCl concentration exceeds 20%, the viscosity of the sample increases due to the high ionic strength value, making it difficult to transfer the analyte from a large amount of sample to the adsorbent (Chen *et al*. 2016, Mousavi *et al*. 2020). Based on this

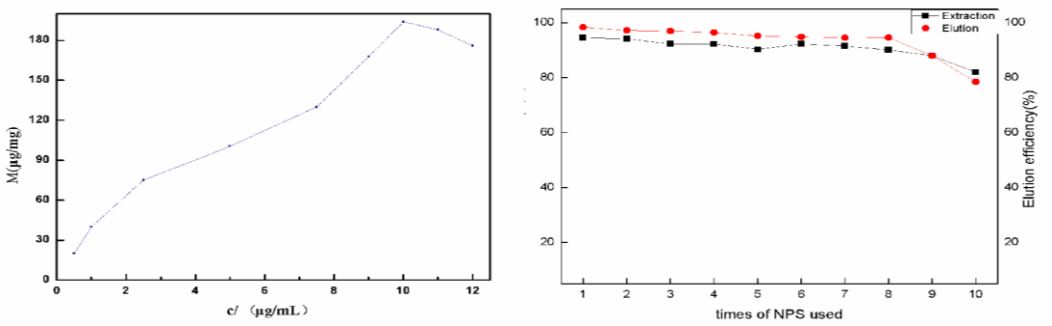

Fig. 12 Adsorption capacity of (a) $CoFe_2O_4$@SiO_2@[BMIM]PF_6 and reusability of the (b) $CoFe_2O_4$@SiO_2 MNPs

Table 2 Comparison of determination methods of trace gold by magnetic solid phase extraction

Element	Magnetic core	Adsorbent	Adsorption capacity(mg·g^{-1})	Cycles	Re.
^{197}Au	Fe_3O_4	Fe_3O_4/SiO_2-SH	43.7	/	[28]
	Fe_3O_4/ SiO_2 / ED	Fe_3O_4/SiO_2/ED	142.9	5	[29]
	Fe_3O_4	Fe_3O_4/SiO_2/cPPyT	845.9	5	[30]
	Fe_3O_4	Compound/Fe_3O_4	47.9	/	[31]
	Fe_3O_4	APT/Fe_3O_4/PANI	/	/	[32]
	Fe_3O_4	Fe_3O_4/Resin	5.78 mmol / g	5	[33]
	Fe_3O_4	Chitosan/$Fe3O_4$	59.52	/	[34]
	$CoFe_2O_4$@SiO_2	$CoFe_2O_4$@SiO_2@[BMIM]PF_6	194	8	This work

result, no electrolyte was added during the extraction (Zou *et al*. 2019, Abedini *et al*. 2020c).

3.2.3 Effect of oscillation time

The effect of oscillation time on the extraction rate was studied (Fig. 10(c)). The results show that after 3 minutes of shaking, the extraction equilibrium can be reached, and the extraction rate is greater than 90%. Therefore, the optimal shaking time is 3 minutes (Wang *et al*. 2020e, Zheng *et al*. 2020).

3.2.4 Amount of extractant

In order to understand the influence of $CoFe_2O_4$@SiO_2@[BMIM]PF_6 composite material dosage on the magnetic solid phase extraction process, 1-25mg $CoFe_2O_4$@SiO_2@[BMIM]PF_6 composite material was studied. The results are shown in Fig. 10(d). With the increase of the amount of extractant, the extraction rate gradually increased (Chen *et al*. 2019, Cao 2020, Gholipour *et al*. 2020b). When the amount of extraction was 20mg, the extraction rate reached the maximum (Abedini *et al*. 2019, Liu *et al*. 2020d). After that, if the amount of extractant was increased, the extraction rate no longer increased. Therefore, in the magnetic solid phase extraction process, the most suitable amount of $CoFe_2O_4$@SiO_2@[BMIM]PF_6 composite material is 20 mg.

3.3 Optimization of gold (III) elution

The influence of eluent selected, eluent concentration, eluent volume and elution time on the elution effect was investigated (Cui *et al*. 2021, Zhang *et al*. 2021). The results showed that 0.5% thiourea + 1 mol·L^{-1} 3ml 20min reached the best elution, and the elution rate was above 90%.

3.3.1 Eluent selected

As shown in Fig. 11(a), the gold (III) elution efficiency of 0.5% thiourea + 1 mol·L^{-1} was increased to 96%.

3.3.2 Effect of eluent concentration

Effect of eluent volume on the elution efficiency of thiourea was evaluated in the range of 0-3.0%. The efficiency of thiourea was above 85% from 0.1% to 5.0%, and reached more than 95% in 0.5%. Therefore, 0.5% thiourea + 1 mol·L^{-1} hydrochloric acid solution was chosen as eluent (Fig. 11(b)).

3.3.3 Effect of eluent volume

Effect of eluent volume on the elution efficiency of thiourea was evaluated in the range of 3.0-8.0 mL ($CoFe_2O_4$@SiO_2@[BMIM]PF_6 MNPs 0.1 g). The efficiency of thiourea was above 85% from 1.5 mL to 5.0 mL, and reached more than 95% in 3.0 mL. The preconcentration factor was 10-fold (the quotient of volume before absorption and after elution) (Wang *et al*. 2020d, Zhang *et al*. 2020g). The optimum volume of ethanol was chosen at 3.0 mL as shown in Fig. 11(c).

3.3.4 Effect of elution time

As could been in Fig. 11(d), the elution efficiency was increased up to 95% after 3 min of stripping time used. Thereafter, 3 min of elution time was selected for further studies (Zhang *et al*. 2019c, Wang *et al*. 2020c).

3.4 Adsorption capacity

Table 3 Determination of gold content in various water samples ($\mu g \cdot L^{-1}$)

Water sample source	Waterworks of Shengli road	Dayang Zhuang	Waterworks of West Ganyu city	Siying	Qiantan	Waterworks of Haizhou	Drainage of mine plant	Hot spring of Donghai
Position of resources	119°13'7.47"E 34°36'44.63"N	119°13'7.47"E 34°36'44.63"N	119°13'7.47"E 34°36'44.63"N	119°13'7.47"E 34°36'44.63"N	119°13'7.93"E 34°36'45.39"N	119°13'7.05"E 34°36'45.77"N	119°13'7.84"E 34°36'44.82"N	119°13'7.84"E 34°36'44.82"N
Content ($\mu g \cdot L^{-1}$)	0.002	0.003	0.002	0.003	0.004	0.004	0.318	0.020
%RSD	2.15	1.25	3.12	2.11	1.55	2.56	2.4	1.5
Recovery rate (%)			108.0-112.3					

*Gold Standard Sample for Water Testing BWB2233-2016

Table 4 Recovery rate experiment of gold (III) gold standard sample for water sample testing (n = 3)

Element	Source of water sample	Background value/μg	Scalar addition/μg	Recovery value/μg	Recovery rate/%
^{127}Au	Qiantan	1.416	0.300	1.744	109.3
	Waterworks of Maokou	1.996	0.300	2.312	105.3
	Waterworks of Haizhou	2.017	0.300	2.341	108.0
	Waterworks of West Ganyu city	1.686	0.300	2.023	112.3

Adsorption capacity is defined as the maximum amount of gold (III) adsorbed per gram of $CoFe_2O_4@SiO_2@[BMIM]PF_6$. In this work the adsorption capacity of gold (III) for $CoFe_2O_4@SiO_2@[BMIM]PF_6$ was studied through changing gold (III) concentration in aqueous samples before MSPE procedure (Yang *et al*. 2015, Zhang *et al*. 2020f). When the concentration of gold (III) was 10.0 $\mu g \cdot mL^{-1}$, the adsorption of gold (III) reached the maximum. The adsorption capacity for $CoFe_2O_4@SiO_2@[BMIM]PF_6$ was calculated as 194 $mg \cdot g^{-1}$, which showed the better adsorption capacity of $CoFe_2O_4@SiO_2@[BMIM]PF_6$ for gold (III) as shown in Fig. 12(a). (Tu *et al*. 2011, Marwani *et al*. 2012, Behbahani *et al*. 2013, 2014, Chen *et al*. 2015, Ghorbani-Kalhor *et al*. 2015, Awual 2016, Hyder *et al*. 2018).

3.5 Reusability of the $CoFe_2O_4@SiO_2$ MNPs

In order to investigate the recycling of the $CoFe_2O_4@SiO_2$ MNPs, they were washed with 3 mL 0.5% thiourea for twice after each MSPE run, and subsequently assembled with [BMIM] PF_6 ionic liquid. Each prepared adsorbent was used for MSPE (Wang *et al*. 2020a, b). The experimental results were shown in Fig. 12(b). It was clear that no obvious loss of the sorption capacity occurred after 8 times of recycling. These results indicated that the self-assembly did not influence the stability of the $CoFe_2O_4@SiO_2$ MNPs for reusability (Wang *et al*. 2020a, Xu *et al*. 2020a).

3.6 Comparison of method

This magnetic solid phase extraction-ICP-MS method for the determination of trace gold was compared with other magnetic solid phase extraction methods for the determination of gold as below in Table 2.

3.7 Sample determination

$CoFe_2O_4@SiO_2@[BMIM]PF_6$ MNPs were successfully prepared and applied as magnetic adsorbents to preconcentrate and separate gold (III) in water sample. The prepared MNPs have an extraction capacity of 194 $mg \cdot g^{-1}$, a detection limit of 0.002 $\mu g \cdot L^{-1}$, and a linear range of 0.01 to 1000 $\mu g \cdot L^{-1}$, which can be reused more than 8 times. The content of gold in water sample was determined by this MSPE combined with ICP-MS (Yang *et al*. 2020a, Yu *et al*. 2020a) method. The results of the analyzed certified reference materials are within the allowable error range of the standard values (RSD % < 5%). The gold content in water samples from seven drinking water sources in Lianyungang was analyzed and the contents was varying between 0.002 and 0.3 $\mu g \cdot L^{-1}$(Table 3.).

3.8 Recovery rate experiment

10 $\mu g \cdot L^{-1}$ gold (III) standard solution was used as the standard solution, 0.1, 1, 10 $\mu g \cdot L^{-1}$ standard solution was added. The results are shown in Table 4.

Recovery rate of gold (III) content in different samples was between 96.0% and 112.3%, which was in accordance with GB/T23942-2009.

3.9 Preliminary study on adsorption mechanism

3.9.1 Adsorption kinetics experiment

The kinetic experiments of $CoFe_3O_4@SiO_2@[BMIM]PF_6$ on gold (III)show that the adsorption is a pseudo-second-order kinetic model, which shows that the adsorption is multi-layer adsorption, mainly chemical adsorption, and the adsorption process is exothermic and spontaneous (Jia *et al*. 2020a, Zhang *et al*. 2020k). Langmuir model is more suitable to describe the adsorption

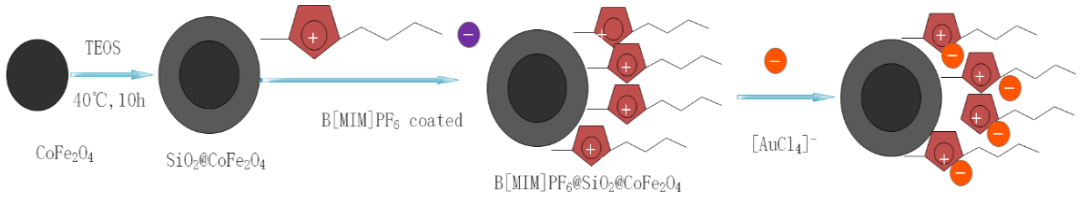

Fig. 14 The chemical structure of gold in HCl solution and the mechanism of removal gold (III) by $CoFe_2O_4@SiO_2@$ [BMIM]PF_6

behavior of adsorbent in this work, which belongs to multi-layer adsorption. This is consistent with Bet's experiment (Abedini *et al*. 2020a, Sun *et al*. 2020a).

3.9.2 Adsorption morphology of gold (III)

The adsorption morphology of gold (III) during the adsorption process was investigated by $[AuCl_4]$ absorption spectra (Fig. 13). The curves a, b, c, d are the adsorption spectra of $[AuCl_4]^-$ system before adsorption, adsorption phase after adsorption, adsorbed phase and blank control respectively. It can be seen from Fig. 13 that the ionic liquid [BMIM]PF_6 has no characteristic absorption peak at 315nm, while $[AuCl_4]$ has characteristic absorption peak at 315nm before adsorption. The adsorption phase retained the characteristic absorption of $[AuCl_4]^-$, indicating that gold (III) was adsorbed into [BMIM]PF_6 ionic liquid phase in form of $[AuCl_4]^-$. It is described that the preparation process of the new nano-materials and the process of adsorbing trace gold in Fig. 14.

4. Conclusions

A new magnetic nano adsorbent $CoFe_2O_4@SiO_2@$ [BMIM]PF_6 was prepared. It was confirmed by SEM, TEM, EDS, XRD, FTIR, TGA and VSM methods that the ionic liquid C_4MIM $[PF_6]$ was self-assembled into $CoFe_2O_4@SiO_2$. The tested element gold (III) was rapidly adsorbed on the composite nano adsorbent of $CoFe_2O_4@SiO_2@$[BMIM] PF_6 and eluted with thiourea. The kinetic experiments shows that the adsorption is a pseudo-second-order kinetic model. Langmuir model is more suitable to describe the adsorption behavior of adsorbent in this work, which belongs to multi-layer adsorption. This method has been successfully applied to the determination of gold in water samples.

Acknowledgments

This study was supported by the Postgraduate Research and Practice Innovation Program of Jiangsu Province (CXZZ13_0892, China); National Youth Science Fund Project (31300652, 41706141, China); the funding of Open subject of Jiangsu Institute of Marine Resources Development; the funding of Jiangsu Ocean University Youth Fund (kx15039, China); the funding of Practical Innovation Project for college students of Huaihai Institute of Technology (PICX132, China).

References

Abedini, M. and Zhang, C. (2020a), "Blast performance of concrete columns retrofitted with FRP using segment pressure technique", *Compos. Struct.*, **2020**, 113473. https://doi.org/10.1016/j.compstruct.2020.113473.

Abedini, M. and Zhang, C. (2020b), "Performance assessment of concrete and steel material models in LS-DYNA for enhanced numerical simulation, a state of the art review", *Arch. Comput. Methods Eng.*, **2020**, 1-22. https://doi.org/10.1007/s11831-020-09483-5.

Abedini, M., Mutalib, A.A., Mehrmashhadi, J., Raman, S.N., Alipour, R., Momeni, T. and Mussa, M.H. (2019), "Large deflection behavior effect in reinforced concrete columns exposed to extreme dynamic loads", *Front. Struct. Civ. Eng.*, **14**(2), 532-553. https://doi.org/10.1007/s11709-020-0604-9.

Abedini, M., Zhang, C., Mehrmashhadi, J. and Akhlaghi, E. (2020c), "Comparison of ALE, LBE and pressure time history methods to evaluate extreme loading effects in RC column", *Structures*, **28**, 456-466. https://doi.org/10.1016/j.istruc.2020.08.084.

Afrazi, M. (2018), "Numerical simulation of soil lateral pressure on flexible retaining walls using a hybrid discrete-finite element method", Ph.D. Dissertation, Tarbiat Modares University, Jalal, Iran.

Afrazi, M. and Dehghani, M. (2014), "Choosing the best route variants base on Environmental parameters by means of remote sensing and GIS", *Proceedings of the 3rd International Conference on Recent Advances in Railway Engineering*, Tehran, Iran, May.

Afrazi, M. and Rouhanifar, S. (2019), "Experimental study on mechanical behavior of sand-rubber mixtures", *Modares Civ. Eng. J.*, **19**(4), 83-96.

Afrazi, M., Mahmoud, Y., Alitalesh, M. and Fakhimi, A.A. (2018a), "Numerical analysis of effective parameters in direct shear test by hybrid discrete - finite element method", *Modares Civ. Eng. J.*, **18**(3), 13-24.

Afrazi, M., Pirjalili, A., Golshani, A.A. and Fakhournezhad, A. (2017), "MATLAB codes for finite element analysis of a tunnel", *Proceeding of the 4th International Conference on Recent Innovations in Civil Engineering, Architecture and Urban Planning*, Tehran, Iran, September.

Afrazi, M., Yazdani, M., Radfar, S. and Rezamand, A. (2018b), "Finite element modelling of the settlement of a foundation under uniform surcharge", *Proceedings of the 4th International Conference on New Developments in Soil Mechanics and Geotechnical Engineering*, North Cyprus, June.

Ahamed, M.A., Reza, M.I. and Al-Amin, M. (2020), "Electricity generation from speed breaker by air compression method using wells turbine", *J. Adv. Eng. Comput.*, **4**(2), 140-148. https://doi.org/10.25073/jaec.202042.277.

Alam, Z., Sun, L., Zhang, C., Su, Z. and Samali, B. (2020a), "Experimental and numerical investigation on the complex behaviour of the localised seismic response in a multi-storey plan-asymmetric structure", *Struct. Infrastruct. Eng.*, **2020**, 1-

17. https://doi.org/10.1080/15732479.2020.1730914.

Alam, Z., Zhang, C. and Samali, B. (2020b), "Influence of seismic incident angle on response uncertainty and structural performance of tall asymmetric structure", *Struct. Des. Tall Special Build.*, **29**(12), e1750. https://doi.org/10.1002/tal.1750.

Alam, Z., Zhang, C. and Samali, B. (2020c), "The role of viscoelastic damping on retrofitting seismic performance of asymmetric reinforced concrete structures", *Earthq. Eng. Eng. Vib.*, **19**(1), 223-237. https://doi.org/10.1007/s11803-020-0558-x.

Alaskar, A., Shah, S., Keerio, M.A., Phulpoto, J.A., Baharom, S., Assilzadeh, H., Alyousef, R., Alabduljabbar, H. and Mohamed, A.M. (2020), "Development of Pozzolanic material from clay", *Adv. Concrete Constr.*, **10**(4), 301-310. https://doi.org/10.12989/acc.2020.10.4.301.

Alaskar, A., Wakil, K., Alyousef, R., Jermsittiparsert, K., Ho, L.S., Alabduljabbar, H., Alrshoudi, F. and Mohamed, A.M. (2020), "Computational analysis of three dimensional steel frame structures through different stiffening members", *Steel Compos. Struct.*, **35**(2), 187-197. https://doi.org/10.12989/scs.2020.35.2.187.

Alyousef, R., Alabduljabbar, H., Mohamed, A.M., Alaskar, A., Jermsittiparsert, K. and Ho, L.S. (2020), "A model to develop the porosity of concrete as important mechanical property", *Smart Struct. Syst.*, **26**(2), 147-156. https://doi.org/10.12989/sss.2020.26.2.147.

Amiri, M., Salavati-Niasari, M., Akbari, A. and Razavi, R. (2017a), "Sol-gel auto-combustion synthesize and characterization of a novel anticorrosive cobalt ferrite nanoparticles dispersed in silica matrix", *J. Mater. Sci. Mater. Electron.*, **28**(14), 10495-10508. https://doi.org/10.1007/s10854-017-6823-8.

Amiri, M., Salavati-Niasari, M., Pardakhty, A., Ahmadi, M. and Akbari, A. (2017b), "Caffeine: A novel green precursor for synthesis of magnetic $CoFe_2O_4$ nanoparticles and pH-sensitive magnetic alginate beads for drug delivery", *Mater. Sci. Eng. C*, **76**, 1085-1093. https://doi.org/10.1016/j.msec.2017.03.208.

Arif, M.Z., Ahmed, R., Sadia, U.H., Tultul, M.S.I. and Chakma, R. (2020), "Decision tree method using for fetal state classification from cardiotography data", *J. Adv. Eng. Comput.*, **4**(1), 64-73. https://doi.org/10.25073/jaec.202041.273.

Awual, M.R. (2016), "Solid phase sensitive palladium (II) ions detection and recovery using ligand based efficient conjugate nanomaterials", *Chem. Eng. J.*, **300**, 264-272. https://doi.org/10.1016/j.cej.2016.04.071.

Aziz-Zanjani, M.O. and Mehdinia, A. (2014), "A review on procedures for the preparation of coatings for solid phase microextraction", *Microchim. Acta*, **181**(11-12), 1169-1190. https://doi.org/10.1007/s00604-014-1265-y.

Bazilevs, Y., Takizawa, K., Tezduyar, T.E., Hsu, M.C., Otoguro, Y., Mochizuki, H. and Wu, M.C.H. (2020), "Wind turbine and turbomachinery computational analysis with the ALE and space-time variational multiscale methods and isogeometric discretization", *J. Adv. Eng. Comput.*, **4**(1), 1-32. https://doi.org/10.25073/jaec.202041.278.

Behbahani, M., Bagheri, A., Gorji, T., Nabid, M.R., Sedghi, R., Oskooie, H.A. and Heravi, M.M. (2013), "Application of poly (N-phenylethanolamine) modified MWCNTs as a new sorbent for solid-phase extraction of trace palladium ions in soil and water samples", *Sample Prep.*, **1**(2013), 10-17. https://doi.org/10.2478/sampre-2013-0002.

Behbahani, M., Najafi, F., Amini, M.M., Sadeghi, O., Bagheri, A. and Hassanlou, P.G. (2014), "Solid phase extraction using nanoporous MCM-41 modified with 3, 4-dihydroxybenz-aldehyde for simultaneous preconcentration and removal of gold (III), palladium (II), copper (II) and silver (I)", *J. Ind. Eng. Chem.*, **20**(4), 2248-2255. https://doi.org/10.1016/j.jiec.2013.09.057.

Cao, L. (2020), "Changing port governance model: Port spatial structure and trade efficiency", *J. Coast. Res.*, **95**, 963-968. https://doi.org/10.2112/SI95-187.1.

Cao, Y., Alyousef, R., Baharom, S., Shah, S., Alaskar, A., Alabduljabbar, H., Mustafa Mohamed, A. and Assilzadeh, H. (2020), "Dynamic attainment of mixed aspect ratio for concrete members reinforced with steel fiber under impact loading", *Mech. Adv. Mater. Struct.*, 1-10. https://doi.org/10.1080/15376494.2020.1847371.

Cao, Y., Fan, Q., Azar, S.M., Alyousef, R., Yousif, S.T., Wakil, K., Jermsittiparsert, K., Ho, L.S., Alabduljabbar, H. and Alaskar, A. (2020), "Computational parameter identification of strongest influence on the shear resistance of reinforced concrete beams by fiber reinforcement polymer", *Struct.*, **27**, 118-127. https://doi.org/10.1016/j.istruc.2020.05.031.

Cao, Y., Wakil, K., Alyousef, R., Jermsittiparsert, K., Ho, L.S., Alabduljabbar, H., Alaskar, A., Alrshoudi, F. and Mohamed, A.M. (2020), "Application of extreme learning machine in behavior of beam to column connections", *Struct.*, **25**, 861-867. https://doi.org/10.1016/j.istruc.2020.03.058.

Cao, Y., Wakil, K., Alyousef, R., Yousif, S.T., Jermsittiparsert, K., Ho, L.S., Alabduljabbar, H., Alaskar, A., Alrshoudi, F. and Mohamed, A.M. (2020), "Computational earthquake performance of plan-irregular shear wall structures subjected to different earthquake shock situations", *Earthq. Struct.*, **18**(5), 567-580. https://doi.org/10.12989/eas.2020.18.5.567.

Chang, S.H. (2020), "Gold (III) recovery from aqueous solutions by raw and modified chitosan: A review", *Carbohydr. Polym.*, **2020**,117423. https://doi.org/10.1016/j.carbpol.2020.117423.

Chen, H., Du, P., Chen, J., Hu, S., Li, S. and Liu, H. (2010), "Separation and preconcentration system based on ultrasonic probe-assisted ionic liquid dispersive liquid-liquid micro-extraction for determination trace amount of chromium (VI) by electrothermal atomic absorption spectrometry", *Talanta*, **81**(1-2), 176-179. https://doi.org/10.1016/j.talanta.2009.11.054.

Chen, J. and Zhu, X. (2015), "Ionic liquid coated magnetic core/shell Fe_3O_4@SiO_2 nanoparticles for the separation/ analysis of linuron in food samples", *Spectrochim. Acta A Mol. Biomol. Spectrosc.*, **137**, 456-462. https://doi.org/10.1016/j.saa.2014.08.113.

Chen, J. and Zhu, X. (2016), "Magnetic solid phase extraction using ionic liquid-coated core-shell magnetic nanoparticles followed by high-performance liquid chromatography for determination of Rhodamine B in food samples", *Food Chem.*, **200**, 10-15. https://doi.org/10.1016/j.foodchem.2016.01.002.

Chen, S., Hassanzadeh-Aghdam, M. and Ansari, R. (2018a), "An analytical model for elastic modulus calculation of SiC whisker-reinforced hybrid metal matrix nanocomposite containing SiC nanoparticles", *J. Alloys Compd.*, **767**, 632-641. https://doi.org/10.1016/j.jallcom.2018.07.102.

Chen, X., Wang, D., Wang, T., Yang, Z., Zou, X., Wang, P., Luo, W., Li, Q., Liao, L. and Hu, W. (2019), "Enhanced photoresponsivity of a GaAs nanowire metal-semiconductor-metal photodetector by adjusting the fermi level", *ACS Appl. Mater. Interf.*, **11**(36), 33188-33193. https://doi.org/10.1021/acsami.9b07891.

Chen, Y., He, L., Guan, Y., Lu, H. and Li, J. (2017), "Life cycle assessment of greenhouse gas emissions and water-energy optimization for shale gas supply chain planning based on multi-level approach: Case study in Barnett, Marcellus, Fayetteville, and Haynesville shales", *Energy Convers. Manag.*, **134**, 382-398. https://doi.org/10.1016/j.enconman.2016.12.019.

Chen, Y., He, L., Li, J. and Zhang, S. (2018b), "Multi-criteria design of shale-gas-water supply chains and production systems towards optimal life cycle economics and greenhouse gas emissions under uncertainty", *Comput. Chem. Eng.*, **109**, 216-

235. https://doi.org/10.1016/j.compchemeng.2017.11.014.
Chen, Y., Li, J., Lu, H. and Yan, P. (2021), "Coupling system dynamics analysis and risk aversion programming for optimizing the mixed noise-driven shale gas-water supply chains", *J. Cleaner Prod*., **278**, 123209. https://doi.org/10.1016/j.jclepro.2020.123209.
Cheng, X., He, L., Lu, H., Chen, Y. and Ren, L. (2016), "Optimal water resources management and system benefit for the Marcellus shale-gas reservoir in Pennsylvania and West Virginia", *J. Hydrol*., **540**, 412-422. https://doi.org/10.1016/j.jhydrol.2016.06.041.
Cui, D., Li, J., Zhang, X., Zhang, L., Chang, H. and Wang, Q. (2021), "Pyrolysis temperature effect on compositions of basic nitrogen species in Huadian shale oil using positive-ion ESI FT-ICR MS and GC-NCD", *J. Anal. Appl. Pyrolysis*, **153**, 104980. https://doi.org/10.1016/j.jaap.2020.104980.
Deng, Y., Zhang, T., Clark, J., Aminabhavi, T., Kruse, A., Tsang, D.C., Sharma, B.K., Zhang, F. and Ren, H. (2020), "Mechanisms and modelling of phosphorus solid-liquid transformation during the hydrothermal processing of swine manure", *Green Chem*., **22**(17), 5628-5638. https://doi.org/10.1039/D0GC01281E.
Deng, Y., Zhang, T., Sharma, B. K. and Nie, H. (2019), "Optimization and mechanism studies on cell disruption and phosphorus recovery from microalgae with magnesium modified hydrochar in assisted hydrothermal system", *Sci. Total Environ*., **646**, 1140-1154. https://doi.org/10.1016/j.scitotenv.2018.07.369.
Dinh-Cong, D., Keykhosravi, M.H., Alyousef, R., Salih, M.N., Nguyen, H., Alabduljabbar, H., Alaskar, A., Alrshoudi, F. and Poi-Ngian, S. (2019), "The effect of wollastonite powder with pozzolan micro silica in conventional concrete containing recycled aggregate", *Smart Struct. Syst.*, **24**(4), 541-552. https://doi.org/10.12989/sss.2019.24.4.541.
Fanaie, N. and Dizaj, E.A. (2014), "Response modification factor of the frames braced with reduced yielding segment BRB", *Struct. Eng. Mech., Int. J.*, **50**(1), 1-17. http://dx.doi.org/10.12989/sem.2014.50.1.001.
Fanaie, N. and Shamlou, S.O. (2015b), "Response modification factor of mixed structures", *Steel Compos. Struct., Int J.*, **19**(6), 1449-1466. https://doi.org/10.12989/scs.2015.19.6.1449.
Fanaie, N., Aghajani, S. and Afsar Dizaj, E. (2016a), "Strengthening of moment-resisting frame using cable-cylinder bracing", *Adv. Struct. Eng.*, **19**(11), 1736-1754. https://doi.org/10.1177/1369433216649382.
Fanaie, N., Aghajani, S. and Dizaj, E.A. (2016b), "Theoretical assessment of the behavior of cable bracing system with central steel cylinder", *Adv. Struct. Eng.*, **19**(3), 463-472. https://doi.org/10.1177/1369433216630052.
Fanaie, N., Aghajani, S. and Shamloo, S. (2012), "Theoretical assessment of wire rope bracing system with soft central cylinder", *Proceedings of the 15th World Conference on Earthquake Engineering*, Lisbon, Portugal, September.
Fanaie, N., Esfahani, F.G. and Soroushnia, S. (2015a), "Analytical study of composite beams with different arrangements of channel shear connectors", *Steel Compos. Struct., Int J.*, **19**(2), 485-501. https://doi.org/10.12989/scs.2015.19.2.485.
Fang, D., Cheng, J., Gong, K., Shi, Q.R., Zhou, X.L. and Liu, Z.L. (2008), "A green and novel procedure for the preparation of ionic liquid", *J. Fluorine Chem.*, **129**(2), 108-111. https://doi.org/10.1016/j.jfluchem.2007.09.004.
Feng, S., Lu, H., Tian, P., Xue, Y., Lu, J., Tang, M. and Feng, W. (2020a), "Analysis of microplastics in a remote region of the Tibetan plateau: Implications for natural environmental response to human activities", *Sci. Total Environ*., **739**, 140087. https://doi.org/10.1016/j.scitotenv.2020.140087.
Feng, W., Lu, H., Yao, T. and Yu, Q. (2020b), "Drought characteristics and its elevation dependence in the Qinghai-Tibet plateau during the last half-century", *Sci. Rep*., **10**(1), 1-11. https://doi.org/10.1038/s41598-020-71295-1.
Ganesan, T., Vasant, P., Sanghvi, P., Thomas, J. and Litvinchev, I. (2020), "Random matrix generators for optimizing a fuzzy biofuel supply chain system", *J. Adv. Eng. Comput*., **4**(1), 33-50. https://doi.org/10.25073/jaec.202041.268.
Gao, N. and Lu, K. (2020), "An underwater metamaterial for broadband acoustic absorption at low frequency", *Appl. Acoust*., **169**, 107500. https://doi.org/10.1016/j.apacoust.2020.107500.
Gao, N., Tang, L., Deng, J., Lu, K., Hou, H. and Chen, K. (2021), "Design, fabrication and sound absorption test of composite porous metamaterial with embedding i-plates into porous polyurethane sponge", *Appl. Acoust*., **175**, 107845. https://doi.org/10.1016/j.apacoust.2020.107845.
Gholipour, G., Zhang, C. and Mousavi, A.A. (2020a), "Nonlinear numerical analysis and progressive damage assessment of a cable-stayed bridge pier subjected to ship collision", *Marine Struct*., **69**, 102662. https://doi.org/10.1016/j.marstruc.2019.102662.
Gholipour, G., Zhang, C. and Mousavi, A.A. (2020b), "Numerical analysis of axially loaded RC columns subjected to the combination of impact and blast loads", *Eng. Struct*., **219**, 110924. https://doi.org/10.1016/j.engstruct.2020.110924.
Ghorbani-Kalhor, E., Behbahani, M. and Abolhasani, J. (2015), "Application of ion-imprinted polymer nanoparticles for selective trace determination of palladium ions in food and environmental samples with the aid of experimental design methodology", *Food Anal. Methods*, **8**(7), 1746-1757. https://doi.org/10.1007/s12161-014-0057-7.
Ha, C.N., Anh-Thy, P.C. and Dibya Jyoti, B. (2018), "A new fuzzy rule based contrast enhancement method using the two-steps automatic clustering algorithm", *J. Adv. Eng. Comput*., **2**(4), 239-250. https://doi.org/10.25073/jaec.201824.214.
Han, X., Zhang, D., Yan, J., Zhao, S. and Liu, J. (2020), "Process development of flue gas desulphurization wastewater treatment in coal-fired power plants towards zero liquid discharge: Energetic, economic and environmental analyses", *J. Cleaner Prod*., **261**, 121144. https://doi.org/10.1016/j.jclepro.2020.121144.
He, L., Chen, Y. and Li, J. (2018a), "A three-level framework for balancing the tradeoffs among the energy, water, and air-emission implications within the life-cycle shale gas supply chains", *Resour. Conserv. Recycl*., **133**, 206-228. https://doi.org/10.1016/j.resconrec.2018.02.015.
He, L., Chen, Y., Zhao, H., Tian, P., Xue, Y. and Chen, L. (2018b), "Game-based analysis of energy-water nexus for identifying environmental impacts during Shale gas operations under stochastic input", *Sci. Total Environ.*, **627**, 1585-1601. https://doi.org/10.1016/j.scitotenv.2018.02.004.
He, L., Shen, J. and Zhang, Y. (2018c), "Ecological vulnerability assessment for ecological conservation and environmental management", *J. Environ. Manag.*, **206**, 1115-1125. https://doi.org/10.1016/j.jenvman.2017.11.059.
He, M., Huang, L., Zhao, B., Chen, B. and Hu, B. (2017), "Advanced functional materials in solid phase extraction for ICP-MS determination of trace elements and their species-a review", *Anal. Chimica Acta*, **973**, 1-24. https://doi.org/10.1016/j.aca.2017.03.047.
Hu, X., Chong, H.Y. and Wang, X. (2019), "Sustainability perceptions of off-site manufacturing stakeholders in Australia", *J. Cleaner Prod*., **227**, 346-354. https://doi.org/10.1016/j.jclepro.2019.03.258.
Hu, Y., Chen, Q., Feng, S. and Zuo, C. (2020), "Microscopic fringe projection profilometry: A review", *Optics Lasers Eng*., **135**, 106192. https://doi.org/10.1016/j.optlaseng.2020.106192.
Huang, J., Alyousef, R., Suhatril, M., Baharom, S., Alabduljabbar,

H., Alaskar, A. and Assilzadeh, H. (2020), "Influence of porosity and cement grade on concrete mechanical properties", *Adv. Concrete Constr.*, **10**(5), 393-402. https://doi.org/10.12989/acc.2020.10.5.393.

Huang, Z., Zheng, H., Guo, L. and Mo, D. (2020), "Influence of the position of artificial boundary on computation accuracy of conjugated infinite element for a finite length cylindrical shell", *Acoust. Australia*, **48**(2), 287-294. https://doi.org/10.1007/s40857-020-00175-5.

Hyder, M.M.Z. and Ochiai, B. (2018), "Selective recovery of Au (III), Pd (II), and Ag (I) from printed circuit boards using cellulose filter paper grafted with polymer chains bearing thiocarbamate moieties", *Microsyst. Technol.*, **24**(1), 683-690. https://doi.org/10.1007/s00542-017-3277-0.

Inoue, K., Gurung, M., Xiong, Y., Kawakita, H., Ohto, K. and Alam, S. (2015), "Hydrometallurgical recovery of precious metals and removal of hazardous metals using persimmon tannin and persimmon wastes", *Metals*, **5**(4), 1921-1956. https://doi.org/10.3390/met5041921.

Jia, L., Liu, B., Zhao, Y., Chen, W., Mou, D., Fu, J., Wang, Y., Xin, W. and Zhao, L. (2020a), "Structure design of MoS_2@Mo_2C on nitrogen-doped carbon for enhanced alkaline hydrogen evolution reaction", *J. Mater. Sci.*, **55**(34), 16197-16210. https://doi.org/10.1007/s10853-020-05107-2.

Jia, L.C., Jin, Y.F., Ren, J., Zhao, L., Yan, D.X. and Li, Z.M. (2021), "Highly thermally conductive liquid metal-based composites with superior thermostability for thermal management", *J. Mater. Chem. C*, **2021**, 1-13. https://doi.org/10.1039/D0TC05493C.

Jia, Q., Huang, S., Hu, M., Song, Y., Wang, M., Zhang, Z. and He, L. (2020b), "Polyoxometalate-derived MoS_2 nanosheets embedded around iron-hydroxide nanorods as the platform for sensitively determining miRNA-21", *Sens. Actuators B Chem.*, **323**, 128647. https://doi.org/10.1016/j.snb.2020.128647.

Jiao, S.Q., Jiao, H.D., Song, W.L., Wang, M.Y. and Tu, J.G. (2020), "A review on liquid metals as cathodes for molten salt/oxide electrolysis", *Int. J. Miner., Metal. Mater.*, **27**, 1588-1598. https://doi.org/10.1007/s12613-020-1971-x.

Jiao, S.Q., Wang, M.Y. and Song, W.L. (2020), "Editorial for special issue on high-temperature molten salt chemistry and technology", *Int. J. Miner., Metal. Mater.*, **27**(12), 1569-1571. https://doi.org/10.1007/s12613-020-2225-7.

Ju, Y., Shen, T. and Wang, D. (2020), "Bonding behavior between reactive powder concrete and normal strength concrete", *Constr. Build. Mater.*, **242**, 118024. https://doi.org/10.1016/j.conbuildmat.2020.118024.

Katebi, J., Shoaei-parchin, M., Shariati, M., Trung, N.T. and Khorami, M. (2019), "Developed comparative analysis of metaheuristic optimization algorithms for optimal active control of structures", *Eng. Comput.*, **2019**, 1-20. https://doi.org/10.1007/s00366-019-00780-7.

Kordestani, H. and Zhang, C. (2020a), "Direct use of the savitzky-golay filter to develop an output-only trend line-based damage detection method", *Sensors*, **20**(7), 1983. https://doi.org/10.3390/s20071983.

Kordestani, H., Zhang, C. and Shadabfar, M. (2020b), "Beam damage detection under a moving load using random decrement technique and Savitzky-Golay filter", *Sensors*, **20**(1), 243. https://doi.org/10.3390/s20010243.

Li, C., Sun, L., Xu, Z., Wu, X., Liang, T. and Shi, W. (2020a), "Experimental investigation and error analysis of high precision FBG displacement sensor for structural health monitoring", *Int. J. Struct. Stab. Dyn.*, **20**(6), 2040011. https://doi.org/10.1142/S0219455420400118.

Li, H., Zhang, T., Tsang, D.C. and Li, G. (2020b), "Effects of external additives: Biochar, bentonite, phosphate, on co-composting for swine manure and corn straw", *Chemosphere*, **248**, 125927. https://doi.org/10.1016/j.chemosphere.2020.125927.

Li, X., Zhang, R., Zhang, X., Zhu, P. and Yao, T. (2020c), "Silver-catalyzed decarboxylative allylation of difluoro-arylacetic acids with allyl sulfones in water", *Chem. Asian J.*, **15**(7), 1175-1179. https://doi.org/10.1002/asia.202000059.

Liu, C., Wu, X., Wakil, K., Jermsittiparsert, K., Ho, L.S., Alabduljabbar, H., Alaskar, A., Alrshoudi, F., Alyousef, R. and Mohamed, A.M. (2020), "Computational estimation of the earthquake response for fibre reinforced concrete rectangular columns", *Steel Compos. Struct.*, **34**(5), 743-767. https://doi.org/10.12989/scs.2020.34.5.743.

Liu, G., Ren, G., Zhao, L., Cheng, L., Wang, C. and Sun, B. (2017), "Antibacterial activity and mechanism of bifidocin against Listeria monocytogenes", *Food Control*, **73**, 854-861.

Liu, H., Liu, X., Zhao, F., Liu, Y., Liu, L., Wang, L., Geng, C. and Huang, P. (2020a), "Preparation of a hydrophilic and antibacterial dual function ultrafiltration membrane with quaternized graphene oxide as a modifier", *J. Colloid Interf. Sci.*, **562**, 182-192. https://doi.org/10.1016/j.jcis.2019.12.017.

Liu, J., Wang, C., Sun, H., Wang, H., Rong, F., He, L., Lou, Y., Zhang, S., Zhang, Z. and Du, M. (2020b), "CoOx/CoNy nanoparticles encapsulated carbon-nitride nanosheets as an efficiently trifunctional electrocatalyst for overall water splitting and Zn-air battery", *Appl. Catal. B Environ.*, **279**, 119407. https://doi.org/10.1016/j.apcatb.2020.119407.

Liu, J., Wu, C., Wu, G. and Wang, X. (2015), "A novel differential search algorithm and applications for structure design", *Appl. Math. Comput.*, **268**, 246-269. https://doi.org/10.1016/j.amc.2015.06.036.

Liu, L., Li, D., Ma, Y., Shen, H., Zhao, S. and Wang, Y. (2020c), "Combined application of arbuscular mycorrhizal fungi and exogenous melatonin alleviates drought stress and improves plant growth in tobacco seedlings", *J. Plant Growth Regul.*, **2020**, 1-14. https://doi.org/10.1007/s00344-020-10165-6.

Liu, L., Li, J., Yue, F., Yan, X., Wang, F., Bloszies, S. and Wang, Y. (2018), "Effects of arbuscular mycorrhizal inoculation and biochar amendment on maize growth, cadmium uptake and soil cadmium speciation in Cd-contaminated soil", *Chemosphere*, **194**, 495-503. https://doi.org/10.1016/j.chemosphere.2017.12.025.

Liu, Y., Hu, B., Wu, S., Wang, M., Zhang, Z., Cui, B., He, L. and Du, M. (2019), "Hierarchical nanocomposite electrocatalyst of bimetallic zeolitic imidazolate framework and MoS_2 sheets for non-Pt methanol oxidation and water splitting", *Appl. Catal. B Environ.*, **258**, 117970. https://doi.org/10.1016/j.apcatb.2019.117970.

Liu, Y., Xu, T., Liu, Y., Gao, Y. and Di, C. (2020d), "Wear and heat shock resistance of Ni-WC coating on mould copper plate fabricated by laser", *J. Mater. Res. Technol.*, **9**(4), 8283-8288. https://doi.org/10.1016/j.jmrt.2020.05.083.

Long, Q., Wu, C. and Wang, X. (2015), "A system of nonsmooth equations solver based upon subgradient method", *Appl. Math. Comput.*, **251**, 284-299. https://doi.org/10.1016/j.amc.2014.11.064.

Lu, H., Guan, Y., He, L., Adhikari, H., Pellikka, P., Heiskanen, J. and Maeda, E. (2020), "Patch aggregation trends of the global climate landscape under future global warming scenario", *Int. J. Climatol.*, **40**(5), 2674-2685. https://doi.org/10.1002/joc.6358.

Lu, H., Tian, P. and He, L. (2019), "Evaluating the global potential of aquifer thermal energy storage and determining the potential worldwide hotspots driven by socio-economic, geo-hydrologic and climatic conditions", *Renew. Sustain. Energy Rev.*, **112**, 788-796. https://doi.org/10.1016/j.rser.2019.06.013.

Lu, Z., Dai, J., Song, X., Wang, G. and Yang, W. (2008), "Facile synthesis of Fe_3O_4/SiO_2 composite nanoparticles from primary silica particles", *Colloids Surf. A Physicochem. Eng. Aspects*, **317**(1-3), 450-456. https://doi.org/10.1016/j.colsurfa.2007.11.020.

Majedi, M., Afrazi, M. and Fakhimi, A. (2020a), "FEM-BPM simulation of SHPB testing for measurement of rock tensile strength", *Proceedings of the 54th US Rock Mechanics / Geomechanics Symposium*, Colorado, USA, July.

Majedi, M.R., Afrazi, M. and Fakhimi, A. (2020b), "A micromechanical model for simulation of rock failure under high strain rate loading", *Int. J. Civ. Eng.*, **2020**, 1-15. https://doi.org/10.1007/s40999-020-00551-2.

Mansouri, I., Shariati, M., Safa, M., Ibrahim, Z., Tahir, M. and Petković, D. (2019), "Analysis of influential factors for predicting the shear strength of a V-shaped angle shear connector in composite beams using an adaptive neuro-fuzzy technique", *J. Intell. Manuf.*, **30**(3), 1247-1257.

Marwani, H.M., Albishri, H.M., Jalal, T.A. and Soliman, E.M. (2012), "Activated carbon immobilized dithizone phase for selective adsorption and determination of gold (III)", *Desalin. Water Treat.*, **45**(1-3), 128-135. https://doi.org/10.1080/19443994.2012.692019.

Mehdinia, A., Jebeliyan, M., Kayyal, T. B. and Jabbari, A. (2017), "Rattle-type Fe_3O_4@SnO_2 core-shell nanoparticles for dispersive solid-phase extraction of mercury ions", *Microchim. Acta*, **184**(3), 707-713. https://doi.org/10.1007/s00604-016-2059-1.

Milovancevic, M., Marinović, J.S., Nikolić, J., Kitić, A., Shariati, M., Trung, N.T., Wakil, K. and Khorami, M. (2019), "UML diagrams for dynamical monitoring of rail vehicles", *Physica A*, **53**, 121169. https://doi.org/10.1016/j.physa.2019.121169.

Moghaddam, H., Fanaie, N. and Hamzehloo, H. (2009), "Uniform hazard response spectra and ground motions for Tabriz", *J. Sci. Iran.*, **16**(3), 238-248.

Mohammadhassani, M., Nezamabadi-Pour, H., Suhatril, M. and Shariati, M. (2013), "Identification of a suitable ANN architecture in predicting strain in tie section of concrete deep beams", *Struct. Eng. Mech., Int. J.*, **46**(6), 853-868. https://doi.org/10.12989/sem.2013.46.6.853.

Mohammadhassani, M., Nezamabadi-Pour, H., Suhatril, M. and Shariati, M. (2014), "An evolutionary fuzzy modelling approach and comparison of different methods for shear strength prediction of high-strength concrete beams without stirrups", *Smart Struct. Syst., Int. J.*, **14**(5), 785-809. https://doi.org/10.12989/sss.2014.14.5.785.

Mou, B., Zhao, F., Qiao, Q., Wang, L., Li, H., He, B. and Hao, Z. (2019), "Flexural behavior of beam to column joints with or without an overlying concrete slab", *Eng. Struct.*, **199**, 109616. https://doi.org/10.1016/j.engstruct.2019.109616.

Mousavi, A.A., Zhang, C., Masri, S.F. and Gholipour, G. (2020), "Structural damage localization and quantification based on a CEEMDAN Hilbert transform neural network approach: A model steel truss bridge case study", *Sensors*, **20**(5), 1271. https://doi.org/10.3390/s20051271.

Nguyen-Thi, K.N., Che-Ngoc, H. and Pham-Chau, A.T. (2020), "An efficient image contrast enhancement method using sigmoid function and differential evolution", *J. Adv. Eng. Comput.*, **4**(3), 162-172. https://doi.org/10.25073/jaec.202043.267.

Pham, N.T., Dang, N.M.D. and Nguyen, S.D. (2021), "A method upon deep learning for speech emotion recognition", *J. Adv. Eng. Comput.*, **4**(4), 273-285. https://doi.org/10.25073/jaec.202044.311.

Pho, K.H. and Truong, B.C. (2020), "Comparison of the performance of the gradient and Newton-Raphson method to estimate parameters in some zero-inflated regression models", *J. Adv. Eng. Comput.*, **4**(4), 227-250. https://doi.org/10.25073/jaec.202044.297.

Qi, C. and Fourie, A. (2019), "Cemented paste backfill for mineral tailings management: Review and future perspectives", *Min. Eng.*, **144**, 106025. https://doi.org/10.1016/j.mineng.2019.106025.

Qi, C., Chen, Q. and Kim, S. (2020), "Integrated and intelligent design framework for cemented paste backfill: A combination of robust machine learning modelling and multi-objective optimization", *Miner. Eng.*, **155**, 106422. https://doi.org/10.1016/j.mineng.2020.106422.

Qi, C., Chen, Q. and Kim, S.S. (2020), "Integrated and intelligent design framework for cemented paste backfill: A combination of robust machine learning modelling and multi-objective optimization", *Min. Eng.*, **155**, 106422. https://doi.org/10.1016/j.mineng.2020.106422.

Qi, C., Fourie, A., Chen, Q. and Liu, P. (2019), "Application of first-principles theory in ferrite phases of cemented paste backfill", *Min. Eng.*, **133**, 47-51. https://doi.org/10.1016/j.mineng.2019.01.011.

Qi, C., Guo, L., Ly, H.-B., Le, H. V. and Pham, B. T. (2021), "Improving pressure drops estimation of fresh cemented paste backfill slurry using a hybrid machine learning method", Minerals Engineering **163**, 106790 DOI: https://doi.org/10.1016/j.mineng.2021.106790.

Qi, C., Spagnoli, D. and Fourie, A. (2020), "DFT-D study of single water adsorption on low-index surfaces of calcium silicate phases in cement", *Appl. Surf. Sci.*, **518**, 146255. https://doi.org/10.1016/j.apsusc.2020.146255.

Qi, C., Spagnoli, D. and Fourie, A. (2020), "Structural, electronic, and mechanical properties of calcium aluminate cements: Insight from first-principles theory", *Constr. Build. Mater.*, **264**, 120259. https://doi.org/10.1016/j.conbuildmat.2020.120259.

Qian, J., Feng, S., Li, Y., Tao, T., Han, J., Chen, Q. and Zuo, C. (2020a), "Single-shot absolute 3D shape measurement with deep-learning-based color fringe projection profilometry", *Opt. Lett.*, **45**(7), 1842-1845. https://doi.org/10.1364/OL.388994.

Qian, J., Feng, S., Tao, T., Hu, Y., Li, Y., Chen, Q. and Zuo, C. (2020b), "Deep-learning-enabled geometric constraints and phase unwrapping for single-shot absolute 3D shape measurement", *APL Photon.*, **5**(4), 046105. https://doi.org/10.1063/5.0003217.

Radi, S., Tighadouini, S., El Massaoudi, M., Hadda, T.B., Zaghrioui, M., Bacquet, M., Dacquin, J. and Warad, I. (2014), "Synthesis of 1-(Pyrrol-2-yl) imine modified silica as a new sorbent for the removal of toxic metals from aqueous solutions", *J. Mater. Environ. Sci.*, **5**, 1280-1287.

Rahimi, Z., Sarafraz, H., Alahyarizadeh, G. and Shirani, A. (2018), "Hydrothermal synthesis of magnetic $CoFe_2O_4$ nanoparticles and $CoFe_2O_4$/MWCNTs nanocomposites for U and Pb removal from aqueous solutions", *J. Radioanal. Nucl. Chem.*, **317**(1), 431-442. https://doi.org/10.1007/s10967-018-5894-1.

Reuter, M. and Van Schaik, A. (2016), "Gold-A key enabler of a circular economy: Recycling of waste electric and electronic equipment", *Gold Ore Process.*, **2016**, 937-958. https://doi.org/10.1016/B978-0-444-63658-4.00053-0.

Rouhanifar, S., Afrazi, M., Fakhimi, A. and Yazdani, M. (2020), "Strength and deformation behaviour of sand-rubber mixture", *Int. J. Geotech. Eng.*, **2020**, 1-15. https://doi.org/10.1080/19386362.2020.1812193.

Roy, S.K., Nayak, D., Dash, N., Dhawan, N. and Rath, S.S. (2020), "Microwave-assisted reduction roasting-magnetic separation studies of two mineralogically different low-grade iron ores", *Int. J. Miner., Metal. Mater.*, **27**(11), 1449-1461. https://doi.org/10.1007/s12613-020-1992-5.

Sadeghipour Chahnasir, E., Zandi, Y., Shariati, M., Dehghani, E., Toghroli, A., Mohamed, E.T., Shariati, A., Safa, M., Wakil, K. and Khorami, M. (2018), "Application of support vector machine with firefly algorithm for investigation of the factors affecting the shear strength of angle shear connectors", *Smart Struct. Syst., Int. J.*, **22**(4), 413-424. http://dx.doi.org/10.12989/sss.2018.22.4.413.

Safa, M., Sari, P.A., Shariat, M., Suhatril, M., Trung, N.T., Wakil, K. and Khorami, M. (2020), "Development of neuro-fuzzy and

neuro-bee predictive models for prediction of the safety factor of eco-protection slopes", *Physica A*, **550**, 124046. https://doi.org/10.1016/j.physa.2019.124046.

Safa, M., Sari, P.A., Shariati, M., Suhatril, M., Trung, N.T., Wakil, K. and Khorami, M. (2020), "Development of neuro-fuzzy and neuro-bee predictive models for prediction of the safety factor of eco-protection slopes", *Physica A: Statist. Mech. Its Appl.*, **550**, 124046. https://doi.org/10.1016/j.physa.2019.124046.

Safa, M., Shariati, M., Ibrahim, Z., Toghroli, A., Baharom, S.B., Nor, N.M. and Petkovic, D. (2016), "Potential of adaptive neuro fuzzy inference system for evaluating the factors affecting steel-concrete composite beam's shear strength", *Steel Compos. Struct., Int. J.*, **21**(3), 679-688. http://dx.doi.org/10.12989/scs.2016.21.3.679.

Sedghi, Y., Zandi, Y., Shariati, M., Ahmadi, E., Moghimi Azar, V., Toghroli, A., Safa, M., Tonnizam Mohamad, E., Khorami, M. and Wakil, K. (2018), "Application of ANFIS technique on performance of C and L shaped angle shear connectors", *Smart Struct. Syst., Int. J.*, **22**(3), 335-340. http://dx.doi.org/10.12989/sss.2018.22.3.335.

Shariati, M., Mafipour, M.S., Ghahremani, B., Azarhomayun, F., Ahmadi, M., Trung, N.T. and Shariati, A. (2020), "A novel hybrid extreme learning machine–grey wolf optimizer (ELM-GWO) model to predict compressive strength of concrete with partial replacements for cement", *Eng. Comput.*, **2020**, 1-23. https://doi.org/10.1007/s00366-020-01081-0.

Shariati, M., Mafipour, M.S., Haido, J.H., Yousif, S.T., Toghroli, A., Trung, N.T. and Shariati, A. (2020), "Identification of the most influencing parameters on the properties of corroded concrete beams using an Adaptive Neuro-Fuzzy Inference System (ANFIS)", *Steel Compos. Struct.*, **34**(1), 155. https://doi.org/10.12989/scs.2020.34.1.155.

Shariati, M., Mafipour, M.S., Mehrabi, P., Ahmadi, M., Wakil, K., Trung, N.T. and Toghroli, A. (2020), "Prediction of concrete strength in presence of furnace slag and fly ash using Hybrid ANN-GA (Artificial Neural Network-Genetic Algorithm)", *Smart Struct. Syst.*, **25**(2), 183. https://doi.org/10.12989/sss.2020.25.2.183.

Shariati, M., Mafipour, M.S., Mehrabi, P., Bahadori, A., Zandi, Y. Salih, M.N., Nguyen, H., Dou, J., Song, X. and Poi-Ngian, S. (2019), "Application of a hybrid artificial neural network-particle swarm optimization (ANN-PSO) model in behavior prediction of channel shear connectors embedded in normal and high-strength concrete", *Appl. Sci.*, **9**(24), 5534. https://doi.org/10.3390/app9245534.

Shariati, M., Mafipour, M.S., Mehrabi, P., Bahadori, A., Zandi, Y. Salih, M.N., Nguyen, H., Dou, J., Song, X. and Poi-Ngian, S. (2019), "Application of a hybrid artificial neural network-particle swarm optimization (ANN-PSO) model in behavior prediction of channel shear connectors embedded in normal and high-strength concrete", *Appl. Sci.*, **9**(24), 5534. https://doi.org/10.3390/app9245534.

Shariati, M., Mafipour, M.S., Mehrabi, P., Zandi, Y., Dehghani, D., Bahadori, A., Shariati, A., Trung, N.T., Salih, M.N. and Poi-Ngian, S. (2019), "Application of Extreme Learning Machine (ELM) and Genetic Programming (GP) to design steel-concrete composite floor systems at elevated temperatures", *Steel Compos. Struct.*, **33**(3), 319-332. https://doi.org/10.12989/scs.2019.33.3.319.

Shariati, M., Trung, N.T., Wakil, K., Mehrabi, P., Safa, M. and Khorami, M. (2019), "Moment-rotation estimation of steel rack connection using extreme learning machine", *Steel Compos. Struct.*, **31**(5), 427-435. https://doi.org/10.12989/scs.2019.31.5.427.

Shen, C.L., Lou, Q., Zang, J.H., Liu, K.K., Qu, S.N., Dong, L. and Shan, C.X. (2020), "Near-infrared chemiluminescent carbon nanodots and their application in reactive oxygen species bioimaging", *Adv. Sci.*, **7**(8), 1903525. https://doi.org/10.1002/advs.201903525.

Shi, M., Wang, B., Shen, Y., Jiang, J., Zhu, W., Su, Y., Narayanasamy, M., Angaiah, S., Yan, C. and Peng, Q. (2020), "3D assembly of MXene-stabilized spinel ZnMn2O4 for highly durable aqueous zinc-ion batteries", *Chem. Eng. J.*, **399**, 125627. https://doi.org/10.1016/j.cej.2020.125627.

Singh, V., Gu, N. and Wang, X. (2011), "A theoretical framework of a BIM-based multi-disciplinary collaboration platform", *Auto. Constr.*, **20**(2), 134-144. https://doi.org/10.1016/j.autcon.2010.09.011.

Stöber, W., Fink, A. and Bohn, E. (1968), "Controlled growth of monodisperse silica spheres in the micron size range", *J. Colloid Interf. Sci.*, **26**(1), 62-69. https://doi.org/10.1016/0021-9797(68)90272-5.

Sun, L., Li, C., Zhang, C., Liang, T. and Zhao, Z. (2019a), "The strain transfer mechanism of fiber bragg grating sensor for extra large strain monitoring", *Sensors*, **19**(8), 1851. https://doi.org/10.3390/s19081851.

Sun, L., Li, C., Zhang, C., Su, Z. and Chen, C. (2018), "Early monitoring of rebar corrosion evolution based on FBG sensor", *Int. J. Struct. Stab. Dyn.*, **18**(8), 1840001. https://doi.org/10.1142/S0219455418400011.

Sun, L., Su, Z., Xia, Y., Zhang, C. and Li, C. (2019b), "Superwide-range fiber bragg grating displacement sensor based on an eccentric gear: Principles and experiments", *J. Aerosp. Eng.*, **32**(1), 04018129. https://doi.org/10.1061/(ASCE)AS.1943-5525.0000960.

Sun, L., Yang, Z., Jin, Q. and Yan, W. (2020a), "Effect of axial compression ratio on seismic behavior of GFRP reinforced concrete columns", *Int. J. Struct. Stab. Dyn.*, **20**(6), 2040004. https://doi.org/10.1142/S0219455420400040.

Sun, Y., Wang, J., Wu, J., Shi, W., Ji, D., Wang, X. and Zhao, X. (2020b), "Constraints hindering the development of high-rise modular buildings", *Appl. Sci.*, **10**(20), 7159.

Takizawa, K., Bazilevs, Y., Tezduyar, T.E. and Korobenko, A. (2020), "Computational flow analysis in aerospace, energy and transportation technologies with the variational multiscale methods", *J. Adv. Eng. Comput.*, **4**(2), 83-117. https://doi.org/10.25073/jaec.202042.279.

Takizawa, K., Bazilevs, Y.E., Tezduyar, T. and Hsu, M.C. (2019), "Computational cardiovascular flow analysis with the variational multiscale methods", *J. Adv. Eng. Comput.*, **3**(2), 366-405. https://doi.org/10.25073/jaec.201932.245.

Tian, P., Lu, H., Feng, W., Guan, Y. and Xue, Y. (2020), "Large decrease in streamflow and sediment load of Qinghai-Tibetan Plateau driven by future climate change: A case study in Lhasa River basin", *Catena*, **187**, 104340. https://doi.org/10.1016/j.catena.2019.104340.

Toghroli, A., Mohammadhassani, M., Suhatril, M., Shariati, M. and Ibrahim, Z. (2014), "Prediction of shear capacity of channel shear connectors using the ANFIS model", *Steel Compos. Struct.*, **17**(5), 623-639. http://dx.doi.org/10.12989/scs.2014.17.5.623.

Toghroli, A., Suhatril, M., Ibrahim, Z., Safa, M., Shariati, M. and Shamshirband, S. (2016), "Potential of soft computing approach for evaluating the factors affecting the capacity of steel–concrete composite beam", *J. Intel. Manuf.*, 1-9. https://doi.org/10.1007/s10845-016-1217-y.

Tran, C.D., Brandstetter, P., Dinh, B.H., Ho, S.D. and Nguyen, M. H.C. (2018a), "Current-sensorless method for speed control of induction motor based on hysteresis pulse width modulation technique", *J. Adv. Eng. Comput.*, **2**(4), 271-280. https://doi.org/10.25073/jaec.201824.213.

Tran, P.M. and Nguyen, N.T. (2018b), "Numerical determination of truncation orders in the correction method for Stokes equations", *J. Adv. Eng. Comput.*, **2**(1), 44-54. https://doi.org/10.25073/jaec.201821.85.

Trung, N.T., Shahgoli, A.F., Zandi, Y., Shariati, M., Wakil, K.,

Safa, M. and Khorami, M. (2019), "Moment-rotation prediction of precast beam-to-column connections using extreme learning machine", *Struct. Eng. Mech.*, **70**(5), 639-647. https://doi.org/10.12989/sem.2019.70.5.639.

Tsai, Y.H., Wang, J., Chien, W.T., Wei, C.Y., Wang, X. and Hsieh, S.H. (2019), "A BIM-based approach for predicting corrosion under insulation", *Auto. Constr.*, **107**, 102923. https://doi.org/10.1016/j.autcon.2019.102923.

Tu, Z., Lu, S., Chang, X., Li, Z., Hu, Z., Zhang, L. and Tian, H. (2011), "Selective solid-phase extraction and separation of trace gold, palladium and platinum using activated carbon modified with ethyl-3-(2-aminoethylamino)-2-chlorobut-2-enoate", *Microchim. Acta*, **173**(1-2), 231-239. https://doi.org/10.1007/s00604-011-0552-0.

Vojoudi, H., Badiei, A., Banaei, A., Bahar, S., Karimi, S., Ziarani, G.M. and Ganjali, M.R. (2017), "Extraction of gold, palladium and silver ions using organically modified silica-coated magnetic nanoparticles and silica gel as a sorbent", *Microchim. Acta*, **184**(10), 3859-3866.

Wang, B., Song, Z. and Sun, L. (2020a), "A review: Comparison of multi-air-pollutant removal by advanced oxidation processes--industrial implementation for catalytic oxidation processes", *Chem. Eng. J.*, **2020**, 128136. https://doi.org/10.1016/j.cej.2020.128136.

Wang, H., Huang, J., Ding, L., Li, D. and Han, Y. (2011), "A facile synthesis of monodisperse $CoFe_2O_4/SiO_2$ nanoparticles", *Appl. Surf. Sci.*, **257**(16), 7107-7112. https://doi.org/10.1016/j.apsusc.2011.03.063.

Wang, J., Liu, M., Chen, T., Chen, J., Ge, W., Fu, Z., Peng, R., Zhai, X. and Lu, Y. (2018a), "Core-shelled mesoporous $CoFe_2O_4$-SiO_2 material with good adsorption and high-temperature magnetic recycling capabilities", *J. Phys. Chem. Solids*, **115**, 300-306. https://doi.org/10.1016/j.jpcs.2017.12.056.

Wang, J., Lu, S., Wang, Y., Li, C. and Wang, K. (2020b), "Effect analysis on thermal behavior enhancement of lithium-ion battery pack with different cooling structures", *J. Energy Storage*, **32**, 101800. https://doi.org/10.1016/j.est.2020.101800.

Wang, M., Hu, M., Hu, B., Guo, C., Song, Y., Jia, Q., He, L., Zhang, Z. and Fang, S. (2019), "Bimetallic cerium and ferric oxides nanoparticles embedded within mesoporous carbon matrix: Electrochemical immunosensor for sensitive detection of carbohydrate antigen 19-9", *Biosens. Bioelectron.*, **135**, 22-29. https://doi.org/10.1016/j.bios.2019.04.018.

Wang, M., Yang, L., Hu, B., Liu, J., He, L., Jia, Q., Song, Y. and Zhang, Z. (2018b), "Bimetallic NiFe oxide structures derived from hollow NiFe Prussian blue nanobox for label-free electrochemical biosensing adenosine triphosphate", *Biosens. Bioelectron.*,**113**, 16-24. https://doi.org/10.1016/j.bios.2019.04.018.

Wang, P., Yao, T., Li, Z., Wei, W., Xie, Q., Duan, W. and Han, H. (2020c), "A superhydrophobic/electrothermal synergistically anti-icing strategy based on graphene composite", *Compos. Sci. Technol.*, **198**, 108307. https://doi.org/10.1016/j.compscitech.2020.108307.

Wang, P., Zhang, X., Duan, W., Teng, W., Liu, Y. and Xie, Q. (2020g), "Superhydrophobic flexible supercapacitors formed by integrating hydrogel with functional carbon nanomaterials", *Chinese J. Chem.*, **2020**, 1-12.

Wang, Q., Liu, B. and Wang, Z. (2020d), "Investigation of heat transfer mechanisms among particles in horizontal rotary retorts", *Powder Technol.*, **367**, 82-96. https://doi.org/10.1016/j.powtec.2020.03.042.

Wang, X.F., Gao, P., Liu, Y.F., Li, H.F. and Lu, F. (2020e), "Predicting thermophilic proteins by machine learning", *Current Bioinform.*, **15**(5), 493-502. https://doi.org/10.2174/1574893615666200207094357.

Wang, X.P., Li, Z.C., Sun, T.C., Kou, J. and Li, X.H. (2020), "Factor analysis on the purity of magnesium titanate directly prepared from seashore titanomagnetite concentrate through direct reduction", *Int. J. Miner., Metal. Mater.*, **27**(11), 1462-1470. https://doi.org/10.1007/s12613-020-1990-7.

Wang, Y., Yao, M., Ma, R., Yuan, Q., Yang, D., Cui, B., Ma, C., Liu, M. and Hu, D. (2020f), "Design strategy of barium titanate/polyvinylidene fluoride-based nanocomposite films for high energy storage", *J. Mater. Chem. A*, **8**(3), 884-917.

Wei, Z., Chen, W., Wang, Z., Li, N., Zhang, P., Zhang, M., Zhao, L. and Qiang, Q. (2020), "High-temperature persistent luminescence and visual dual-emitting optical temperature sensing in self-activated $CaNb_2O_6$: Tb^{3+} phosphor", *J. Am. Ceramic Soc.*, **104**(4), 1750-1759. https://doi.org/10.1111/jace.17579.

Wu, C., Wang, X., Chen, M. and Kim, M.J. (2019), "Differential received signal strength based RFID positioning for construction equipment tracking", *Adv. Eng. Inf.*, **42**, 100960. https://doi.org/10.1016/j.aei.2019.100960.

Wu, C., Wu, P., Wang, J., Jiang, R., Chen, M. and Wang, X. (2020), "Critical review of data-driven decision-making in bridge operation and maintenance", *Struct. Infrastruct. Eng.*, **2020**, 1-24. https://doi.org/10.1080/15732479.2020.1833946.

Wu, C., Wu, P., Wang, J., Jiang, R., Chen, M. and Wang, X. (2021), "Ontological knowledge base for concrete bridge rehabilitation project management", *Auto. Constr.*, **121**, 103428. https://doi.org/10.1016/j.autcon.2020.103428.

Xu, L., Jiang, S. and Zou, Q. (2020a), "An in silico approach to identification, categorization and prediction of nucleic acid binding proteins", *Brief. Bioinform.*, **2020**, 1-13.

Xu, P., Lu, W., Zhang, J. and Zhang, L. (2020b), "Efficient hydrolysis of ammonia borane for hydrogen evolution catalyzed by plasmonic Ag@ Pd core-shell nanocubes", *ACS Sustain. Chem. Eng.*, **8**(33), 12366-12377. https://doi.org/10.1021/acssuschemeng.0c02276.

Xu, S., Wang, J., Shou, W., Ngo, T., Sadick, A.M. and Wang, X. (2020c), "Computer vision techniques in construction: A critical review", *Arch. Comput. Methods Eng.*, **2020**, 1-15. https://doi.org/10.1007/s11831-020-09504-3.

Yang, J., Li, S., Wang, Z., Dong, H., Wang, J. and Tang, S. (2020a), "Using deep learning to detect defects in manufacturing: A comprehensive survey and current challenges", *Materials*, **13**(24), 5755. https://doi.org/10.3390/ma13245755.

Yang, W., Zhao, Y., Wang, D., Wu, H., Lin, A. and He, L. (2020b), "Using principal components analysis and IDW interpolation to determine spatial and temporal changes of surface water quality of Xin'anjiang river in Huangshan, China", *Int. J. Environ. Res. Public Health*, **17**(8), 2942. https://doi.org/10.3390/ijerph17082942.

Yang, Y., Liu, J., Yao, J., Kou, J., Li, Z., Wu, T., Zhang, K., Zhang, L. and Sun, H. (2020c), "Adsorption behaviors of shale oil in kerogen slit by molecular simulation", *Chem. Eng. J.*, **387**, 124054. https://doi.org/10.1016/j.cej.2020.124054.

Yang, Y., Yao, J., Wang, C., Gao, Y., Zhang, Q., An, S. and Song, W. (2015), "New pore space characterization method of shale matrix formation by considering organic and inorganic pores", *J. Natural Gas Sci. Eng.*, **27**, 496-503. https://doi.org/10.1016/j.jngse.2015.08.017.

Yazdani, M., Kabirifar, K., Frimpong, B.E., Shariati, M., Mirmozaffari, M. and Boskabadi, A. (2020), "Improving construction and demolition waste collection service in an urban area using a simheuristic approach: A case study in Sydney, Australia", *J. Clean. Prod.*, **280**, 124138. https://doi.org/10.1016/j.jclepro.2020.124138.

Yu, H., Yang, M., Qian, G., Cai, J., Zhou, H. and Fu, X. (2020a),

"Gradation segregation characteristic and its impact on performance of asphalt mixture", *J. Mater. Civ. Eng.*, **33**(3), 04020478. https://doi.org/10.1016/j.jngse.2015.08.017.

Yu, H., Zhu, X., Qian, G., Gong, X. and Nie, X. (2020b), "Evaluation of phosphorus slag (PS) content and particle size on the performance modification effect of asphalt", *Constr. Build. Mater.*, **256**, 119334. https://doi.org/10.1016/j.conbuildmat.2020.119334.

Zhang, C. and Mousavi, A.A. (2020), "Blast loads induced responses of RC structural members: State-of-the-art review", *Compos. Part B Eng.*, **2020**, 108066. https://doi.org/10.1016/j.compositesb.2020.108066.

Zhang, C. and Wang, H. (2019a), "Robustness of the active rotary inertia driver system for structural swing vibration control subjected to multi-type hazard excitations", *Appl. Sci.*, **9**(20), 4391. https://doi.org/10.3390/app9204391.

Zhang, C. and Wang, H. (2019b), "Swing vibration control of suspended structure using active rotary inertia driver system: Parametric analysis and experimental verification", *Appl. Sci.*, **9**(15), 3144. https://doi.org/10.3390/app9153144.

Zhang, C. and Wang, H. (2020), "Swing vibration control of suspended structures using the active rotary inertia driver system: Theoretical modeling and experimental verification", *Struct. Control Health Monit.*, **27**(6), e2543. https://doi.org/10.1002/stc.2543.

Zhang, C., Abedini, M. and Mehrmashhadi, J. (2020a), "Development of pressure-impulse models and residual capacity assessment of RC columns using high fidelity Arbitrary Lagrangian-Eulerian simulation", *Eng. Struct.*, **224**, 111219. https://doi.org/10.1016/j.engstruct.2020.111219.

Zhang, C., Alam, Z., Sun, L., Su, Z. and Samali, B. (2019a), "Fibre Bragg grating sensor-based damage response monitoring of an asymmetric reinforced concrete shear wall structure subjected to progressive seismic loads", *Struct. Control Health Monit.*, **26**(3), e2307. https://doi.org/10.1002/stc.2307.

Zhang, C., Gholipour, G. and Mousavi, A.A. (2019b), "Nonlinear dynamic behavior of simply-supported RC beams subjected to combined impact-blast loading", *Eng. Struct.*, **181**, 124-142.

Zhang, C., Gholipour, G. and Mousavi, A.A. (2020b), "State-of-the-art review on responses of RC structures subjected to lateral impact loads", *Arch. Comput. Methods Eng.*, **2020**, 1-31. https://doi.org/10.1007/s11831-020-09467-5.

Zhang, D., Han, X., Wang, H., Yang, Q. and Yan, J. (2020c), "Experimental study on transient heat/mass transfer characteristics during static flash of aqueous NaCl solution", *Int. J. Heat Mass Transfer*, **152**, 119543. https://doi.org/10.1016/j.ijheatmasstransfer.2020.119543.

Zhang, F., Zhou, Y., Zhang, Y., Li, D. and Huang, Z. (2020d), "Facile synthesis of sulfur@ titanium carbide Mxene as high performance cathode for lithium-sulfur batteries", *Nanophotonics*, **9**(7), 1-12. https://doi.org/10.1515/nanoph-2019-0568.

Zhang, J. and Liu, B. (2019), "A review on the recent developments of sequence-based protein feature extraction methods", *Curr. Bioinform.*, **14**(3), 190-199. https://doi.org/10.2174/1574893614666181212102749.

Zhang, J., Chen, Q., Sun, J., Tian, L. and Zuo, C. (2020e), "On a universal solution to the transport-of-intensity equation", *Opt. Lett.*, **45**(13), 3649-3652. https://doi.org/10.1364/OL.391823.

Zhang, J., Sun, J., Chen, Q. and Zuo, C. (2020f), "Resolution analysis in a lens-free on-chip digital holographic microscope", *IEEE Trans. Comput. Imaging*, **6**, 697-710. https://doi.org/10.1109/TCI.2020.2964247.

Zhang, R., Jiang, T., Li, F., Li, G., Chen, H. and Li, X. (2020g), "Coordinated bidding strategy of wind farms and power-to-gas facilities using a cooperative game approach", *IEEE Trans. Sustain. Energy*, **11**(4), 2545-2555. https://doi.org/10.1109/TSTE.2020.2965521.

Zhang, T., He, X., Deng, Y., Tsang, D.C., Yuan, H., Shen, J. and Zhang, S. (2020h), "Swine manure valorization for phosphorus and nitrogen recovery by catalytic-thermal hydrolysis and struvite crystallization", *Sci. Total Environ.*, **729**, 138999. https://doi.org/10.1016/j.scitotenv.2020.138999.

Zhang, T., Wu, X., Fan, X., Tsang, D.C., Li, G. and Shen, Y. (2019c), "Corn waste valorization to generate activated hydrochar to recover ammonium nitrogen from compost leachate by hydrothermal assisted pretreatment", *J. Environ. Manag.*, **236**, 108-117. https://doi.org/10.1016/j.jenvman.2019.01.018.

Zhang, T., Wu, X., Li, H., Tsang, D.C., Li, G. and Ren, H. (2020i), "Struvite pyrolysate cycling technology assisted by thermal hydrolysis pretreatment to recover ammonium nitrogen from composting leachate", *J. Cleaner Prod.*, **242**, 118442. https://doi.org/10.1016/j.jclepro.2019.118442.

Zhang, W., Hu, Y., Liu, J., Wang, H., Wei, J., Sun, P., Wu, L. and Zheng, H. (2020j), "Progress of ethylene action mechanism and its application on plant type formation in crops", *Saudi J. Biol. Sci.*, **27**(6), 1667-1673. https://doi.org/10.1016/j.sjbs.2019.12.038.

Zhang, W., Tang, Z., Yang, Y. and Wei, J. (2021), "Assessment of FRP-concrete interfacial debonding with coupled mixed-mode cohesive zone model", *J. Compos. Constr.*, **25**(2), 04021002. https://doi.org/10.1061/(ASCE)CC.1943-5614.0001114.

Zhang, Y., Xu, C., Chen, P., Nahas, Y., Prokhorenko, S. and Bellaiche, L. (2020k), "Emergence of skyrmionium in a two-dimensional CrGe (Se, Te)$_3$ Janus monolayer", *Phys. Rev. B*, **102**(24), 241107. https://doi.org/10.1103/PhysRevB.102.241107.

Zheng, J., Zhang, C. and Li, A. (2020), "Experimental investigation on the mechanical properties of curved metallic plate dampers", *Appl. Sci.*, **10**(1), 269. https://doi.org/10.3390/app10010269.

Zhong, P.F., Lin, H.M., Wang, L.W., Mo, Z.Y., Meng, X.J., Tang, H.T. and Pan, Y.M. (2020), "Electrochemically enabled synthesis of sulfide imidazopyridines via a radical cyclization cascade", *Green Chem.*, **22**(19), 6334-6339. https://doi.org/10.1039/D0GC02125C.

Zhu, H., Shen, Y., Wang, Q., Chen, K., Wang, X., Zhang, G., Yang, J., Guo, Y. and Bai, R. (2017), "Highly promoted removal of Hg (ii) with magnetic $CoFe_2O_4$@SiO_2 core-shell nanoparticles modified by thiol groups", *RSC Adv.*, **7**(62), 39204-39215. https://doi.org/10.1039/C7RA06163C.

Zhu, J., Shi, Q., Wu, P., Sheng, Z. and Wang, X. (2018a), "Complexity analysis of prefabrication contractors' dynamic price competition in mega projects with different competition strategies", *Complexity*, **2018**, 5928235. https://doi.org/10.1155/2018/5928235.

Zhu, J., Wang, X., Chen, M., Wu, P. and Kim, M.J. (2019a), "Integration of BIM and GIS: IFC geometry transformation to shapefile using enhanced open-source approach", *Auto. Constr.*, **106**, 102859. https://doi.org/10.1016/j.autcon.2019.102859.

Zhu, J., Wang, X., Wang, P., Wu, Z. and Kim, M.J. (2019b), "Integration of BIM and GIS: Geometry from IFC to shapefile using open-source technology", *Auto. Constr.*, **102**, 105-119. https://doi.org/10.1016/j.autcon.2019.02.014.

Zhu, J., Wu, P., Chen, M., Kim, M.J., Wang, X. and Fang, T. (2020a), "Automatically processing IFC clipping representation for BIM and GIS integration at the process level", *Appl. Sci.*, **10**(6), 2009. https://doi.org/10.3390/app10062009.

Zhu, L., Kong, L. and Zhang, C. (2020b), "Numerical study on hysteretic behaviour of horizontal-connection and energy-dissipation structures developed for prefabricated shear walls", *Appl. Sci.*, **10**(4), 1240. https://doi.org/10.3390/app10041240.

Zhu, L., Zhang, C., Guan, X., Uy, B., Sun, L. and Wang, B.

(2018b), "The multi-axial strength performance of composited structural BCW members subjected to shear forces", *Steel Compos. Struct., Int. J.*, **27**(1), 75-87. https://doi.org/10.12989/scs.2018.27.1.075.

Zou, Q., Xing, P., Wei, L. and Liu, B. (2019), "Gene2vec: Gene subsequence embedding for prediction of mammalian N6-methyladenosine sites from mRNA", *RNA*, **25**(2), 205-218. https://doi.org/10.1261/rna.069112.118.

Zuo, C., Chen, Q., Gu, G., Feng, S., Feng, F., Li, R. and Shen, G. (2013), "High-speed three-dimensional shape measurement for dynamic scenes using bi-frequency tripolar pulse-width-modulation fringe projection", *Opt. Lasers Eng.*, **51**(8), 953-960. https://doi.org/10.1016/j.optlaseng.2013.02.012.

Zuo, C., Chen, Q., Tian, L., Waller, L. and Asundi, A. (2015), "Transport of intensity phase retrieval and computational imaging for partially coherent fields: The phase space perspective", *Opt. Lasers Eng.*, **71**, 20-32. https://doi.org/10.1016/j.optlaseng.2015.03.006.

Zuo, C., Sun, J., Li, J., Zhang, J., Asundi, A. and Chen, Q. (2017), "High-resolution transport-of-intensity quantitative phase microscopy with annular illumination", *Sci. Rep.*, **7**(1), 1-22. https://doi.org/10.1038/s41598-017-06837-1.

AT